Southeast Climate Adaptation Science Center Administrative Cover Page

Principal Investigators:

Ken W. Krauss (lead), USGS Wetland and Aquatic Research Center, 700 Cajundome Blvd, Lafayette, Louisiana 70506, USA; phone, +1-337-266-8882; kraussk@usgs.gov

Judith Z. Drexler, USGS California Water Science Center, 6000 J. Street, Placer Hall, Sacramento, California 95819, USA; phone, +1-530-400-7900; jdrexler@usgs.gov

Karen M. Thorne, USGS Western Ecological Research Center, One Shields Avenue, University of California, Davis, California 95616, USA; phone, +1-916-502-2996; kthorne@usgs.gov

Emily J. Pindilli, USGS Science and Decision Center, National Center, 12201 Sunrise Valley Drive, Reston, Virginia 20192, USA; phone, +1-703-648-5732; epindilli@usgs.gov

Eric J. Ward, USGS Wetland and Aquatic Research Center, 700 Cajundome Blvd, Lafayette, Louisiana 70506, USA; phone, +1-337-593-5815, eward@usgs.gov

Project title: Mangrove Habitat Persistence and Carbon Vulnerability Associated with Increased Nutrient Loading and Sea-level Rise at Ding Darling National Wildlife Refuge (Sanibel Island, Florida, USA)

Agreement number: SECASC-0049

Date of report: 1 October 2023

Period of performance: 10/1/2019 to 9/30/2021 (no cost extension to 10/30/2023)

Total funding: $323,680

Public summary: Ding Darling National Wildlife Refuge, on the Southwest Coast of Florida (USA), has extensive mangrove forests that provide wildlife habitat, erosion control, and wave attenuation for Sanibel Island. Sanibel Island has a tourist-based economy with thousands of people visiting annually and influencing the island's ecology. Threats to the mangrove resource are a concern and include limited inland migration routes for mangroves to accommodate rising sea levels, perennial impoundment, and persistent nutrient loading from the Caloosahatchee River. To investigate the influence that current and future nitrogen (N) and phosphorus (P) additions from the river may have on mangrove persistence, scientists exposed mangrove forests in fringe locations (immediately adjacent to the edge of open water) and basin locations (inland of open water) to experimental nutrient additions. The study was conducted over three years and tracked nutrient influences on mangrove soil surface elevation change, soil and emergent root greenhouse gas fluxes, individual tree water use, and leaf-scale water use efficiencies. These data contributed to an understanding of what nutrients can have on

mangrove persistence with rising sea levels and what role nutrients will play in carbon sequestration. Indeed, greater eutrophication may create additional vulnerabilities to mangrove submergence, especially to basin mangroves where P concentrations are high and already reducing soil surface elevations. Greater P loading may also lead to increased losses of dissolved carbon to the open estuary through lateral fluxes as soils mineralize carbon. Thus, results suggest that reducing current P inputs to Sanibel Island's mangroves are management options to consider. Finally, while Sanibel Island's mangroves appear resilient to current rates of sea-level rise for the time-being, any accelerations in sea-level or additional stresses to the forests could lead to rapid mangrove retreat and areal loss.

Southeast Climate Adaptation Science Center Project SECASC-0049

Mangrove Habitat Persistence and Carbon Vulnerability Associated with Increased Nutrient Loading and Sea-level Rise at Ding Darling National Wildlife Refuge (Sanibel Island, Florida, USA)[1]

Ken W. Krauss,[2] Jeremy R. Conrad,[3] Jamie A. Duberstein,[4] Eric J. Ward,[2] Judith Z. Drexler,[5] Kevin J. Buffington,[6] Karen M. Thorne,[6] Brian W. Benscoter,[7,8] Haley Miller,[4] Natalie T. Faron,[7] Sergio L. Merino,[2] Andrew S. From,[2] Elitsa Peneva-Reed,[9] and Zhiliang Zhu[9]

Technical Summary

J.N. "Ding" Darling National Wildlife Refuge (DDNWR) is located on Sanibel Island along the southwestern coast of Florida, USA. Sanibel Island is heavily developed, but DDNWR provides protection for a large mangrove area that supports biodiversity and recreational opportunity. However, nitrogen (N) and phosphorus (P) eutrophication attributed to agriculture discharge along the Caloosahatchee River has affected the area's aquatic habitat with algal blooms and may be causing untimely degradation of Sanibel's mangrove forests. We launched a series of studies to understand how additional nutrient loading to the levels expected in the future might affect DDNWR's mangrove resource. We experimentally fertilized selected mangrove forest areas with N fertilizer (+N; NH_4) and P fertilizer (+P; P_2O_5) for three years, and monitored soil surface elevation change, soil and pneumatophore CO_2 fluxes from respiration, mangrove tree sap flow from two species (*Avicennia germinans*, *Rhizophora mangle*), and individual tree and stand water use, from which we developed carbon (C) budgets for +N and +P vs. control simulations as applied to DDNWR's 1112 ha mangrove area. Many of the measured response variables provided hints of subtle changes in response to +P rather than +N, which were compounded when scaled. From this, we found that additional P loading is expected to stimulate CO_2 uptake via net ecosystem exchange of C, likely pressing the system beyond metabolic capacity and leading to a projected 41% increase in lateral C export to the estuary. Additional lateral C export is concomitant to a reduction in vertical soil surface elevation with +P. Furthermore, an inability of DDNWR's mangroves to bury additional P and a release of P-bound ions to lateral export may exacerbate estuarine eutrophication. We also modelled the effect of sea-level rise influences on DDNWR's mangroves through 2100 using a soil cohort model (WARMER-Mangroves) and found that the mangroves may be resilient to current rates of sea-level rise into the future but may also be susceptible to moderate

[1] Bureau Approval Date (Cooperator Report): 1 October 2023 (**IP-156801**)
[2] U.S. Geological Survey, Wetland and Aquatic Research Center, Lafayette, Louisiana, USA
[3] U.S. Fish and Wildlife Service, Inventory and Monitoring Program, Sanibel Island, Florida, USA
[4] Clemson University, Baruch Institute of Coastal Ecology and Forest Science, Georgetown, South Carolina, USA
[5] U.S. Geological Survey, California Water Science Center, Sacramento, California, USA
[6] U.S. Geological Survey, Western Ecological Research Center, Davis, California, USA
[7] Florida Atlantic University, Department of Biological Sciences, Davie, Florida, USA
[8] U.S. Department of Energy, Earth and Environmental Systems Science Division, Germantown, MD, USA
[9] U.S. Geological Survey, Land Management Research Program, Reston, Virginia, USA

accelerations. Greater eutrophication could create additional vulnerabilities to mangrove submergence, especially to basin mangroves where P concentrations are high and already reducing soil surface elevations in some mangroves. Our results suggest that amelioration of current P concentrations and avoidance of additional P loading to Sanibel Island's mangroves are management options to consider.

Introduction

Mangroves occupy an area of up to 137,600 km^2 globally (Giri and others, 2011; Bunting and others, 2018), where they provide important ecosystem services to humans. Services to residents in south Florida, USA include aesthetics, storm protection, seafood provisioning, recreational fishing, and bird watching. The U.S. Department of the Interior is entrusted with protecting and enhancing many of these ecosystem services on public lands, while exploring emergent value enhancement for society. In recent years, a concerted scientific effort has been directed toward understanding how biological carbon (C) sequestration can be enhanced as an ecosystem service on managed lands through directed activities (Krauss and others, 2022b). Sanibel Island provides a challenging location where residential development, barrier island ecology, mangrove ecosystem health, tropical cyclones, and federal land management intersect, with all future aspects of management threatened to some degree by sea-level rise. For mangroves, sea-level rise resiliency and carbon sequestration are biologically entwined (McKee and others, 2007; Rogers and others, 2019).

The majority of Sanibel Island's long-term biological C sequestration occurs in the perennially wet intertidal soils (that is, in lieu of aboveground woody plant material). Indeed, while saltmarshes and seagrasses also bury C at comparable rates to mangroves (Mcleod and others, 2011), woody plant structure and long-term resilience of mangroves to sea-level rise (Krauss and others, 2014) make them intriguing ecosystems for directing a balance between management activities (such as, hydrologic manipulations), enhancement of C storage, and improvement of other ecosystem services.

Additional ecosystem services, such as nutrient burial (for example, up to 24 g N m^2/yr; Cormier and others, 2022) and denitrification, are provided by mangrove ecosystems lining bays and built environments. While mangroves are active in filtering nutrients from municipal loading, there are threshold concentrations in the sensitivity of mangroves to specific nutrients (Reef and others, 2010), beyond which forest structural health and C sequestration might become compromised and decades of peat building might even collapse, oxidize, and release stored C. Drivers of mangrove ecosystem collapse can be subtle, with recent management attention focusing on preemptive identification of the stressors to prevent habitat collapse and ameliorating potential losses in advance of mass mangrove mortality and massive C release (Lewis and others, 2016). The interplay of mangrove and terrestrial habitat with rising seas has received little attention as a management tool; options are most limited on islands.

Mangroves provide the most immediate value to U.S. citizens in the State of Florida, where the U.S. Department of the Interior manages thousands of hectares of mangroves between Everglades and Biscayne National Parks and multiple National Wildlife Refuges. While cover estimates are variable, mangroves occupy between 1,618 and 2,023 km^2 of intertidal habitat in Florida (Florida FWC, 2005), ranging from the sub-tropical regions of the Everglades and Keys to warm temperate locations at Cedar Key and St. Augustine. Furthermore, mangroves in Florida have comparable rates of C storage to those reported globally, with created wetlands colonized by mangroves in the Tampa Bay area storing 218 g C/m^2/yr within the upper soil horizon alone (Osland and others, 2012). Natural mangroves of the Everglades store 151-393 g C/m^2/yr (Smoak and others, 2013).

Understanding the standing C stocks with eutrophication and sea-level rise, as well as exploring management actions that might influence the rate of loss or gain among those C stocks, are the primary research needs addressed by this project. We focus specifically in J.N. "Ding" Darling National Wildlife Refuge (DDNWR) located on Sanibel Island adjacent to the City of Ft. Myers, Florida. Through a series of

integrated studies targeting mangrove soil surface elevation change, long-term soil C storage, soil and aerial root CO_2 flux, tree sap flow, and leaf-scale water use efficiencies, we describe the influence that additional loading of nitrogen (N) and phosphorus (P) from the Caloosahatchee River might have on mangrove carbon budgets and sea-level rise vulnerability of the refuge's mangrove resource. From these data, we model stand water use, estimate net ecosystem exchange of atmospheric C through a novel approach, develop a refuge-scale C budget and define associated threats, calibrate a tidal wetland sea-level rise model (WARMER-Mangroves), and provide an estimate of projected mangrove area change and C loss/gain through the year 2100.

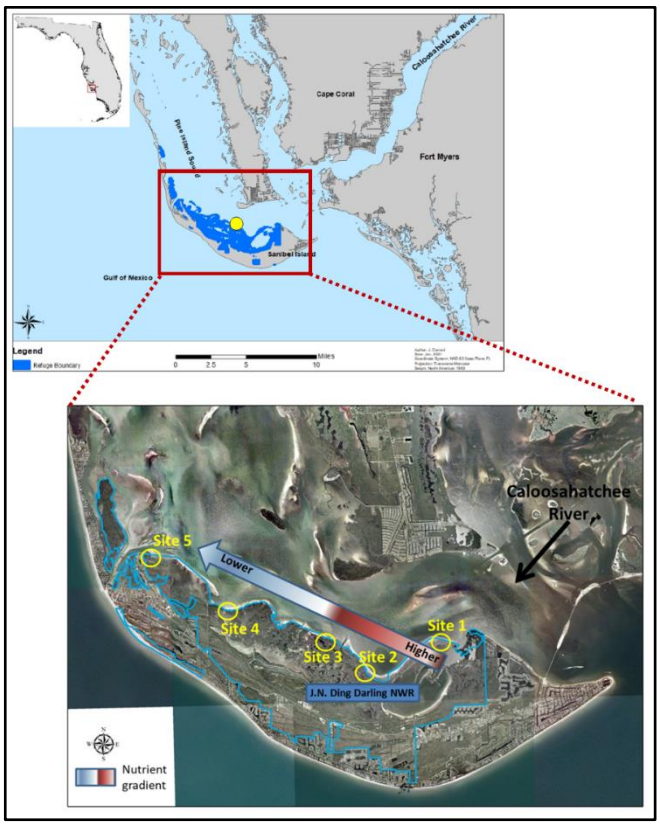

Figure 1. Ding Darling NWR on Sanibel Island, Ft. Myers, Florida along with our originally hypothesized gradient of nitrogen (N) and phosphorus (P) in the mangroves from the Caloosahatchee River.

Threats to the Mangroves of Ding Darling NWR

DDNWR was established in 1945, and covers approximately 2,571 ha of primarily open water, beach strand, and estuarine habitat, including large areas of mangrove forest (**fig. 1**). DDNWR is part of the Southwest Florida Refuge Complex, managed by the U.S. Fish and Wildlife Service along with Matlacha Pass NWR, Pine Island NWR, Island Bay NWR, Caloosahatchee NWR, Florida Panther NWR, and Ten Thousand Islands NWR. Wildlife habitat management is the complex's primary responsibility, as DDNWR and associated islands represent the majority of non-developed habitat on Sanibel Island. In fact, designated wilderness still makes up 44% of DDNWR. Mangrove species present on Sanibel Island include *Rhizophora mangle*, *Avicennia germinans*, and *Laguncularia racemosa*, with one associate, *Conocarpus erectus*, occupying slightly higher elevations along landward edges. Four primary threats exist to this resource, including hurricanes, restricted tidal flows (impoundments), nutrient loading, and migration barriers.

Sanibel Island was impacted by winds and surge of Hurricane Charley (Category 4 storm) in August 2004, with moderate to catastrophic damage sustained by the mangrove forests (Meyers and others, 2006; Milbrandt and others, 2006); this was repeated in 2022 by Hurricane Ian, with damage assessment underway. Thus, structural legacies of damage are pervasive here as in many Caribbean-region mangrove forests (Krauss and Osland, 2018). However, recovery of Sanibel Island's mangroves has proceeded more slowly than expected since 2004 (Peneva-Reed and others, 2021).

Second, while most of DDNWR contains natural tidal mangroves, the refuge does have two rather large impoundments that are managed for water birds. Impoundments are typically drawn down twice per year, once in the Spring and once in the Fall (Meyers and others, 2006). Impoundment management in this fashion can influence tree growth patterns (Lahmann, 1988), potentially influence how C is sequestered, stored, or conveyed across the landscape (Drexler and others, 2013), affect hurricane

recovery (Krauss and others, 2023), and even make mangrove wetlands more susceptible to sea-level rise (Lewis and others, 2016).

The third threat to the mangroves of DDNWR is the Everglades Agricultural Area (EAA). The EAA is located along the southern edges of Lake Okeechobee, produces numerous truck crops, and has a down-stream influence on the mangroves at DDNWR. A system of canals originates from Lake Okeechobee through portions of the EAA to form the Caloosahatchee Canal, which flows westward to become the Caloosahatchee River, dumping into San Carlos Bay and Pine Island Sound adjacent to DDNWR. This canal-river-bay system has and will continue to realize an increase in nutrient loading (NO_x, PO_4) over the coming decades (Liu and others, 2009; Buzzelli and others, 2014), potentially affecting the mangroves of Sanibel.

The fourth threat to the mangroves of DDNWR is the lack of migration corridors for mangrove wetland expansion inland with sea-level rise. The majority of barrier islands in south Florida are developed, which can cause destruction of mangroves through hardening of natural tidal creeks and construction of new navigation canals for boat access to houses. For example, Marco Island, just to the south of Sanibel, lost ~1100 ha of mangrove between 1952 and 1984 (or 24%) (Patterson, 1986), and much of what remains currently is categorized as unhealthy (Krauss and others, 2018a). Furthermore, in-situ production from belowground roots and sediment-entrapping aerial roots stimulates vertical expansion of soils in response to sea-level rise (McKee, 2011). Mangroves respond to rising seas actively, and even if they do not always build vertically at the same rate as locally relevant sea-level rise, some measure of vertical soil expansion is necessary for inland mangrove migration.

Study Approach

Preliminary Sampling

We hypothesized that persistent loading of nitrogen (N) and phosphorus (P) to DDNWR's mangroves was resulting in a shift in the energetics of the ecosystem, potentially affecting mangrove ecosystem respiration, atmospheric exchange of water and C, and soil surface elevation. This, we surmised, was reducing mangrove recovery potential after hurricanes. However, the likelihood that increased nutrient loading was resulting in chronic mangrove ecosystem collapse was of even greater concern. Up to 32% of the nutrients found in the Caloosahatchee watershed come from Lake Okeechobee, 48% of the nutrients come from the non-tidal basin area, and 20% of the nutrients come from the tidal basin area (Lee County 2019). These eutrophic outflows can adversely affect the natural resources in the Caloosahatchee estuary system, including the many habitats represented at DDNWR. Mangroves in south Florida are generally oligotrophic, and it is uncertain what a shift to chronic eutrophication might mean. In order to verify soil nutrient status, we began this project by collecting soil samples along the immediate boundary of mangrove and estuarine waters actively receiving Caloosahatchee River waters.

From the outset of the project, we divided DDNWR's mangroves into two primary types: basin and fringe. Nutrient biogeochemistry, particularly that of P, is particularly sensitive to hydrogeomorphology (Krauss and others, 2006). Fringe mangroves line the edges of bays and backswamp settings of DDNWR and occupy mid-tidal ranges around mean sea-level (MSL) and receive near-daily tidal exchange. Basin mangroves occur just inland of the fringe, are flooded during spring tide or high rainfall events, and hold water for short periods of time commensurate with intertidal pulsing and drainage. These distinctions were established for south Florida mangroves in the 1970's (Lugo and Snedaker, 1974), and apply well to DDNWR.

During preliminary sampling, we discovered that while N concentrations were within the range found among other south Florida mangrove wetlands, soil P concentrations were 3-4 times higher in

some cases and did not track our hypothesized nutrient gradient (Conrad, 2022). P concentrations were also 4 times higher in the basin zone compared to the fringe resulting in an inverse nutrient gradient compared to the oligotrophic mangrove forests of the Florida Everglades, Belize, and Mexico (Chen and Twilley, 1999; Castañeda-Moya and others, 2011; Feller and others, 2002). From this, we began to revise our understanding of the threat to DDNWR mangroves as potentially coming from too much P and altered N:P ratios in lieu of N.

Experimental Design

We conducted long-term fertilization experiments to learn more about past, present, and future nutrient influences on the mangroves at DDNWR. Our experimental design consisted of three locations (blocks) positioned a minimum of 250 m apart (**fig. 2**). Each block was oriented perpendicular to the shoreline and included both hydrogeomorphic zones (fringe and basin) separated by a carbonate ridge. Each block consisted of six, 8 x 8 m process plots, with three plots in each zone positioned a minimum of 25 m from adjacent process plots for a total of 6 plots per block x 3 blocks, or 18 experimental plots (treatment combinations).

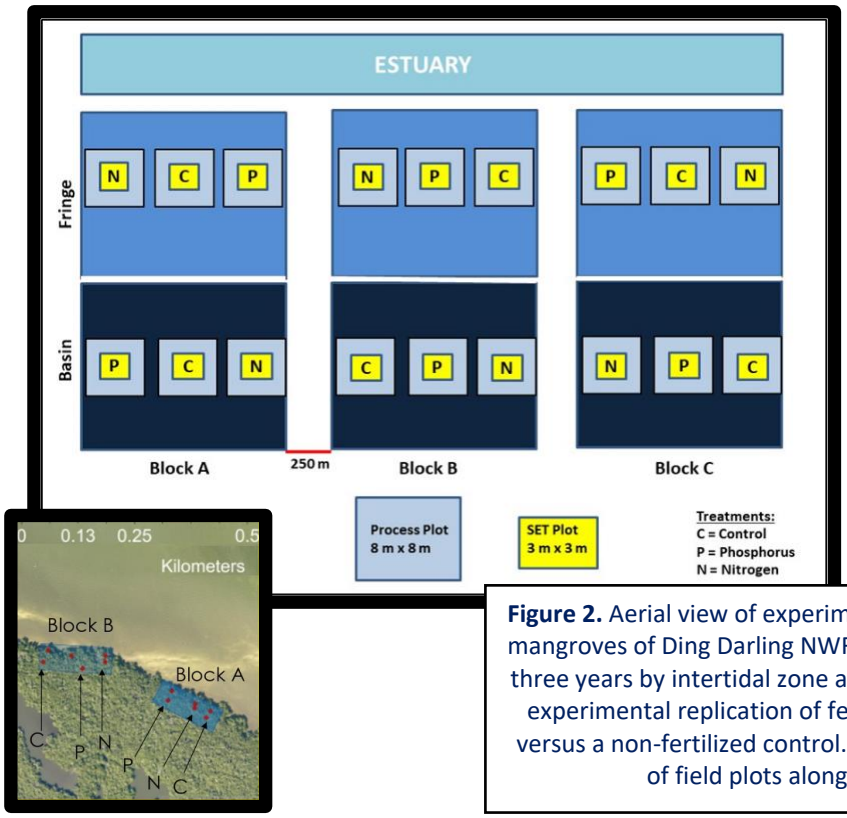

Figure 2. Aerial view of experimental treatments applied to the mangroves of Ding Darling NWR. Treatments were imposed for three years by intertidal zone and consisted of a split-plot with experimental replication of fertilization treatments (+N, +P) versus a non-fertilized control. The inset depicts actual layout of field plots along Pine Island Sound.

Nutrient Treatment/Fertilization Application

To ensure a consistent delivery of nutrients, process plots were randomly assigned one of three nutrient treatments: +N, +P, or control (no amendment). The process plots were fertilized with granular nitrogen (urea NH_4 – 45:0:0, N-P-K) or phosphorus (superphosphate P_2O_5 – 0:45:0, N-P-K) using previously described fertilization methods (Feller 1995; McKee and others, 2002; Feller and others, 2003; McKee and others, 2007). Urea $CO(NH_2)_2$ was used because it readily converts to ammonium (NH_4) which is the primary form of mineralized nitrogen found in mangrove soils (Feller, 1995).

Holes were dug and distributed at 2 m regular grid intervals totaling 16 fertilization holes per plot. These holes have an effective fertilization radius of 1 m (Feller and others, 2003), which we verified through repetitive porewater sampling on Sanibel Island (Miller, 2022). Holes were created using a 2.5 cm diameter auger device to a depth of 30 cm. Once the hole was excavated, 150 g of fertilizer was

inserted within the active root zone and the excavated soil was returned. Hole locations within the plot remained the same for the duration of the experiment. Holes were also created for control plots, but no fertilizer was inserted. Fertilizers were applied twice annually for three years (2018-2020).

Response Variables

We evaluated mangrove response to experimental nutrient addition in several ways, all of which targeted aspects of the C budget (Alongi, 2009). First, we evaluated how soil surface elevations responded with fertilization using the Surface Elevation Table – Marker Horizon (SET-MH) method. Soil compaction or root zone expansion are prominent process drivers of soil C dynamics, and the SET-MH method tracks elevation change and enables differentiation of surface accretion, subsidence, compaction, and root zone expansion (McKee and others, 2007). Second, we measured soil CO_2 fluxes, and separately, pneumatophore CO_2 fluxes from *Avicennia germinans*, a prominent species on all sites. Collectively, these CO_2 flux measurements include soil respiration, belowground live root respiration, above ground live root tissue respiration, and any directing of respiratory CO_2 from deeper soil layers to the atmosphere (Faron, 2021). Third, we measured individual tree sap flow at multiple radial depths into the sapwood of both *A. germinans* and *Rhizophora mangle* occurring in basin mangroves and adjacent fringe areas. Our primary radial sapwood evaluation depth was 5 mm, since that depth would include sap flow through new sapwood developing during fertilization treatments. However, we also measured sap flow to 15, 50, 70, and 90 mm into the sapwood to establish radial depth profiles by treatment in order to determine how tree and stand water use was influenced by fertilization (Krauss and others, 2007; Zhao and others, 2018). Finally, we calibrated a sea-level rise model, WARMER-Mangroves, for application to DDNWR, and ran simulations of projected mangrove habitat change through 2100.

Methods

Along with details provided below, additional references that describe procedures used are reported in **Appendix 1** (**Table 1-1**).

Surface Elevation Table – Marker Horizon (SET-MH)

The SET-MH approach makes use of a deep benchmark rod that is inserted to refusal and from which repetitive time-series measurements of wetland soil surface elevation change is tracked (Cahoon and others, 2002; Callaway and others, 2013). Refusal depth for Sanibel Island's mangroves was 8.0 ± 0.5 m (mean ± SE). During each field measurement, up to 9 pins are extended to the soil surface at the exact same location (direction) created by a fixed attachment of a table device to the rods. Four directions were established for each SET at DDNWR, for a total of up to 36 pin readings during each measurement. At times, individual pins were obscured by roots or large woody debris. A total of three SETs were established per treatment; one in each experimental plot. In all, 18 SETs were installed, and split equally among experimental treatment (+N, +P, control) and between hydrogeomorphic zone (basin, fringe). Associated with the very first reading made at each SET, we established 3 MHs using powdered feldspar clay (Cahoon and Reed, 1995), for a total of 54 MH plots across treatment and zone. Measurements allow us to differentiate surface elevation change (SEC), surface vertical accretion of sediments (VA), shallow subsidence/compaction (SEC < VA), and root zone expansion (SEC > VA). SET-MH plots were re-measured quarterly over the 3 study years at low tide.

Accumulation of soil carbon in the surface sediments can also be determined using either SET or MH data. While previous applications make use of SEC data to determine decadal rates of soil surface carbon accumulation (Lovelock and others, 2014a; Cormier and others, 2022), MH data approximately isolate accumulation of C deposited during fluvial sedimentation over annual time periods of rapid deposition and erosion (Noe and others, 2016). Soil deposited atop MH layers (0-2 cm) were analyzed for carbon, adjusted by bulk density, scaled by area, and combined with VA data to determine surface sediment C accumulation. These data represent transient C accumulation and are distinctive from long-term soil C burial (sediment cores).

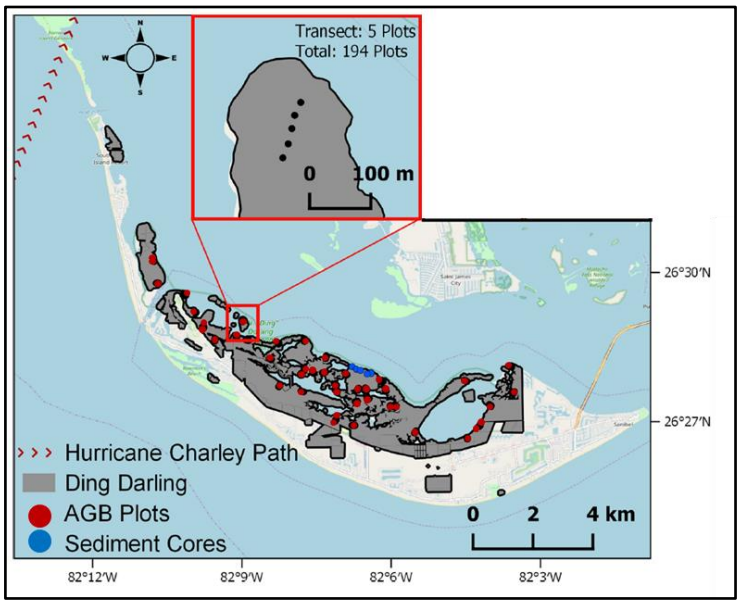

Figure 3. Location of aboveground forest plots established as part of blue carbon stock surveys (Peneva-Reed and others, 2021) and sediment cores analyzed for carbon content and long-term soil C accretion (carbon burial).

Sediment Cores

Sediment cores were extracted from DDNWR to determine how much carbon is stored currently and accumulated in mangrove sediments over long time scales (decades). A total of six cores were taken, three each from basin and fringe environments. Cores were extracted near established study plots (**fig. 3**), and all cores were representative of control treatments since they pre-dated experimental +N and +P treatments. Cores were taken to a depth of 1-m, sectioned into 2-cm segments, and analyzed for bulk density (g/cm^3) and C content (%). Sections were analyzed for ^{137}Cs and ^{210}Pb in order to date the mangrove sediments by depth (Drexler and others, 2013). The Constant Rate of Supply, or CRS model, was used to assign dates to the core profile and determine long-term accretion rates. These data represent long-term soil C burial.

Soil and Pneumatophore CO_2 Fluxes

Soil CO_2 fluxes across the soil surface, which includes microbial soil respiration and live root respiration from the rhizosphere, were measured using a portable infrared gas analyzer (model Li-8100a, Li-Cor Environmental, Inc., Lincoln, NE, USA). Chambers for soil CO_2 flux were 20-cm diameter (or 314 cm^2) and were devoid of aerial roots during in-situ measurements over 4 days each in June (wet season) and November (dry season) of 2020. Control, +N, and +P treatments had 10, 4, and 4 collars, respectively, for a total of 18 collars, spaced at least 0.7-m apart. Collars were inserted to a depth of 0.5 cm and allowed to sit for at least 30 minutes prior to sampling. We oversampled the control for greater power in assessing background soil CO_2 fluxes for NEE_c determinations (see later); it was critical that we were able to develop soil CO_2 flux relationships with air/soil temperature for control plots for use in modeling. These measurements were subsequently repeated. Soil temperature and moisture were measured during soil CO_2 flux measurements with dedicated probes (models Omega soil T probe and Delta-T soil moisture probe, Li-Cor Environmental, Inc., Lincoln, NE, USA).

CO_2 fluxes through pneumatophores of *Avicennia germinans*, which were the prominent aerial root type in basin mangrove forests, were also measured in-situ using a different type of infrared gas analyzer (model EGM-4, PP Systems, Inc., Amesbury, MA, USA). The gas analyzer was attached by Nalgene tubing to gas ports on a 1.3-cm diameter PVC chamber. The chamber fit over an individual pneumatophore, was inserted in the soil at the base of the pneumatophore and was sealed with a latex skirt on top to isolate pneumatophore tissue response. Volume and surface area of the pneumatophore were determined, and fluxes adjusted. Three pneumatophores were sampled from each treatment combination coincident with the timing of soil CO_2 flux measurements.

Data were transformed to a CO_2 flux rate per unit area of soil and converted from molar units to mass (g CO_2/m^2/hour), and then to carbon values. Carbon represents 27.301% of CO_2, and the conversion generates units of g C/m^2/hour.

Sap flow

Sap flow studies were initiated one year after fertilization began using thermal dissipation probes (TDP) connected to voltage regulators and data loggers (model CR1000, Campbell Scientific, Logan, UT, USA). This protocol uses temperature differentials (*d*T) to quantify the flow of sap water within a tree at a specific depth of sapwood. Our systems were configured commercially (model FLGS-TDP, Dynamax, Inc., Houston, TX, USA), and each consisted of 20 wires connected to 32 TDP pairs for *d*T determinations (see Granier, 1987 for theory). We deployed three FLGS-TDP systems. The 32 *d*T pairs were pre-configured to measure sapwood depths of 5 mm (8-12 *d*T sensors), 15 mm (8-12), 50 mm (4), 70 mm (4), and 90 mm (4). Sapwood depths of 5 and 15 mm were interchangeable on the FLGS-TDP systems, as long as voltages were adjusted. Because we hypothesized that changes in sap flow would be most evident at the sapwood depths formed during fertilization, we prioritized 5 mm depths. Growth of DDNWR's mangrove trees ranged from 0.8 to 1.2 cm^2/year of basal area during fertilization periods (Conrad, 2022), corresponding well to our target sapwood depths.

We measured sap flow in *Avicennia germinans* (*dbh*, 6.1-40.9 cm) and *Rhizophora mangle* (*dbh*, 6.7-32.6 cm) trees occupying our experimental sites. The third mangrove species in south Florida, *Laguncularia racemosa*, was not present in sufficient quantities to include. Raw data for sap flow determination are *d*T values, which we recorded over two summers and one winter. Data from every sensor were recorded at 30-minute intervals, and *d*T data were converted to sap flow rates (g H_2O m^2/s, often designated as J_s) relative to the insertion depth using formulas first described by Granier (1987). Data are conveyed as a point sample but on a sapwood area basis and are thus required to be adjusted based on functional sapwood area defined by our radial depth assessments that, along with depths of 5 and 15 mm, include 50, 70, and 90 mm radial sapwood depths at DDNWR.

Analyses were restricted to fair weather, growing season days to avoid confounding environmental conditions (sensu Krauss and others, 2007), as follows: 6 May to 25 June 2019 (32 days used) and 20 June to 21 August 2020 (39 days used). The non-growing season period assessed, corresponding with the end of the northern hemisphere winter, was from 6 February to 22 March 2020.

A partial weather station was deployed approximately 5 km from sap flow studies, and recorded air temperature (°C), relative humidity (%), photosynthetic photon flux density (µmol/m^2/s), barometric pressure (MPa), and rainfall (mm). A second weather station, maintained by DDNWR staff on Sanibel Island was used as a source of radiation data (W/m^2), and supplemental air temperature and rainfall data. These stations were used to determine vapor pressure deficit (*D*); *D* and sap flow are strongly correlated in most sap flow investigations (Bovard and others, 2005). We confirmed that *D*-to-sap flow relationships at DDNWR also provided reliable predictions for scaling purposes (**fig. 1-1**).

Stand Water Use

Sap flow measurements were converted to individual tree water use (*F*) through an individual-based spreadsheet modeling approach that compartmentalizes data from each tree, size class, and species-specific maximum average sap flow (J_s) rate into the following formula (Krauss and others, 2015b),

$$F = \sum_{i=1}^{n} \left(Js_1 \times SA_i \times \frac{Js_i}{Js_1} \right) \quad [1]$$

where *i* is radial depth into the sapwood, 1 is the first depth into the sapwood, Js_1 is sap flow at the first depth, SA_i is the cross-sectional individual tree sapwood area measured by the TDP probe at the *i*-th depth, and the quotient of Js_i/Js_1 is the attenuation of sap flow with radial depth into the tree relative to sap flow at the first depth. All data are reported relative to *i* of 15 mm for scaling because that is the depth of closest adherence to original wattage requirements specified by Granier (1987). The function Js_i/Js_1 was determined separately for control, +N, and +P treatments. Maximum J_s and radial attenuation data for *L. racemosa* were attained from a previous study on sites close to DDNWR (~58 km; Rookery Bay Reserve) (Krauss and others, 2007), and were treated as control values for all simulations.

Calculations of *F* by species and *dbh* were applied to data collected from 128, 7-m-radius plots previously surveyed (Peneva-Reed and others, 2021), but by avoiding plots with heavy Hurricane Charley damage. Raw species and *dbh* data are provided by Peneva-Reed and Zhu (2019), with data collection spanning all of the mangrove habitats of DDNWR (**fig. 3**). Determinations of *F* were converted to stand water use (*S*) by using a biometric model (Čermák and others, 2004; McLaughlin and others, 2012), modified for forested wetlands (Krauss and others, 2015b), as follows,

$$S = \frac{\sum_{i=1}^{n} (F_{\text{tree}})_i}{A} \times \frac{1}{\rho} \quad [2]$$

where *i* corresponds to individual trees in a stand for which *F* is determined by Equation 1, 1 is the first tree in a stand over a diameter limit of ≥ 0.1 cm, 2 is the second tree (etc…), *A* is the ground area occupied by the stand surveyed (m^2), and ρ is the density of water (0.998 g/cm^3). In all, a total of 18,600 lines of calculations were necessary for each of the three simulations of control, +N, and +P at DDNWR. Among each plot, basal area data were collected over a ground area of 153.86 m^2 for trees ≥ 5.0 cm *dbh* and 12.57 m^2 for trees ≥ 0.1 cm but < 5.0 cm. Thus, *S* is reported as kg H_2O/m^2 ground area, which is identical to the same value in millimeters (mm).

Gross Primary Productivity (GPP) and Net Ecosystem Exchange of Carbon (NEE_c)

We estimated NEE_c by first developing a relationship between *S* and gross primary productivity (GPP), or rather the total amount of C taken up by the mangrove canopy in the form of CO_2 based upon the amount of water the canopy used in 2019 and 2020. This is determined using species-specific leaf-scale instantaneous water use efficiencies (WUE_i), which scale reasonably well from leaf-to-canopy using various techniques (Linderson and others, 2012; Liang and others, 2022), and provide a molar accounting of CO_2 taken up per unit water used. We used WUE_i of 3.82, 4.57, and 5.15 mmol CO_2/mol H_2O for *Avicennia germinans*, *Laguncularia racemosa*, and *Rhizophora mangle*, respectively (Krauss, 2004).

However, we were curious as to whether WUE_i might differ by nutrient treatment applied to each study plot at DDNWR. Therefore, we measured WUE_i in-situ using an infrared gas analyzer (model Li-6800, Li-Cor Environmental, Inc., Lincoln, NE, USA) during a mid-summer campaign in August of 2020 on new, but fully extended leaves of control, +N-treated, and +P-treated *A. germinans* and *R. mangle* trees. For these measurements, we held humidity constant in order to maximize WUE_i to force potential differences among species to appear if possible. Species x treatment interactions were not significant ($p > 0.05$), so we collapsed this interaction. Neither species ($F_{1,16} = 0.2688$, $p = 0.611$) nor treatment ($F_{2,16} = 1.82$, $p = 0.193$) differences were significant, indicating that WUE_i likely did not require further consideration as a point of eco-physiological distinction created by +N and +P treatments versus controls. For modeling, the default WUE_i values from Krauss (2004) were used because humidity maintenance by the Li-6800 forced unusually high WUE_i readings in our attempt to maximize potential differences.

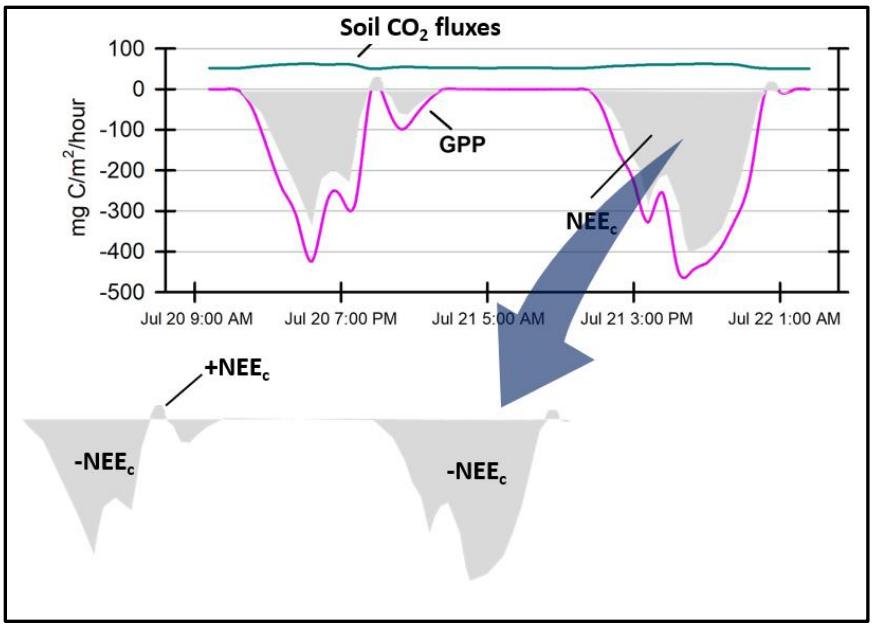

Figure 4. Example calculation of NEE_c from soil CO_2 flux (respiration) and gross primary productivity (GPP) for two study days, as $\int_0^x f'(t)dt$, where (+) NEE_c values represent CO_2 loss and (-) NEE_c values represent CO_2 uptake. NEE_c is the net ecosystem exchange of carbon; NEE_c = GPP – respiration (eq. 3).

WUE_i adjustments were applied to annual values of *S* by species and hydrogeomorphic zone (basin, fringe); $S \propto$ GPP by the relationship of WUE_i. Because each of the 128, 7-m-radius plots had a different basal area distribution by species (Peneva-Reed and others, 2021), we weighted estimates of *S* by species during calculations of GPP using the proportional contribution of individual species to *S* for each plot (**Table 1-2**). Data were transformed to a CO_2 canopy uptake rate and converted from molar units to mass (g CO_2/m^2/hour), and then to C values (g C/m^2/hour), allowing for calculations of NEE_c when combined with soil and pneumatophore CO_2 flux rates, as follows (**fig. 4**),

$$NEE_c = GPP - respiration \quad [3]$$

where respiration is the sum of soil and pneumatophore CO_2 fluxes associated with soil, dead belowground root, and live belowground root respiration. Stem, branch, and coarse woody debris respiration were not included in this value; however, we also made no adjustment for basal area or downed wood occupation of soils to partially compensate. Open ground soil flux differentials would not be large relative to fluxes from woody debris (Troxler and others, 2015). Methane fluxes were also not included but are generally very low from wetlands with salinity > 18 psu (Poffenbarger and others, 2011; Holm and others, 2016). Mean salinity of basin and fringe plots at DDNWR was 46 and 35 psu,

respectively (Conrad, 2022). However, eutrophication can stimulate decomposition and lead to greater methane emissions in some anaerobic environments (Beaulieu and others, 2019), but potential influences were not included here.

Procedurally, determining NEE_c using our chosen method (**fig. 4**) was tested in only one location to date against an eddy covariance (EC) tower (Krauss and others, 2022a). EC procedures directly measure the flux of atmospheric CO_2 into and out of a vegetated canopy using micrometeorological techniques and are generally accepted as representative under many conditions (Baldocchi, 2003). However, EC incurs large establishment and maintenance costs, has a relatively large footprint extending beyond the majority of experimental treatment areas, and has a requirement for gap filling a large number of data points during periods of friction velocity violation. Comparison of EC to our approach in mangroves along the Shark River in Everglades National Park yielded a 0.02 - 0.21 kg C/m^2/year discrepancy, equating to 2.0 - 17.5% of EC measurements (Krauss and others, 2015a; Krauss and others, 2022a). Application can use some improvement, which we contribute for DDNWR by including seasonal variation in estimation of soil and pneumatophore CO_2 fluxes.

As the area of mangroves at DDNWR has been previously mapped as 1112 ± 116 ha (Peneva-Reed and others, 2021), we scale fluxes of water as *S*, as well as carbon as GPP, soil and pneumatophore C fluxes, soil C burial, and surface sediment C accumulation (from SET studies) from the full area of DDNWR's mangroves, dividing basin and fringe occupation equally. From these data, we can estimate export/import of lateral fluxes of particulate organic carbon (POC), dissolved organic carbon (DOC), and dissolved inorganic carbon (DIC) en masse, as follows (Krauss and others, 2018b),

$$(C_{in} - C_{out}) = C_{E/I} + C_B \quad [4]$$

where C_{in} represents all of the measured C entering the mangrove, C_{out} represents all of the measured C exiting the mangrove, $C_{E/I}$ represents the lateral flux mass balance of C, and C_B represents soil C burial. Furthermore, NEE_c approximates the term, ($C_{in} - C_{out}$). With this technique, we cannot differentiate among proportions of the POC, DOC, and DIC as lateral fluxes. We determine how +N and +P treatments might affect C budgets over the study years of 2019 and 2020 relative to control environments.

Sea-level Rise Modeling and the Carbon Resource

Theory and background for WARMER-Mangroves is provided in greater detail in **Appendix 2**. Sea-level rise records and projections for south Florida are constantly being revised by iterative data collection. Among recent empirical analyses, the highest indicates a large acceleration from 3.9 mm yr^{-1} (1900-2021) to contemporary rates of 9.4 mm yr^{-1} (2010-2021) (Parkinson and Wdowinski, 2022). Using these endpoints, we chose four future scenarios encompassing Representative Concentration Pathways (RCPs) from the IPCC AR6 report that project 54 cm (low), 70 cm (medium), 80 cm (medium-high), and 88 cm (high) of sea-level rise for southwest Florida by 2100, relative to the year 2020 (**fig. 5**). The low scenario starts with a 6.1 mm yr^{-1} increase in SLR but declines over the century to 5.33 mm yr^{-1}. The medium scenario projects a 7.3 mm yr^{-1} increase in SLR in 2020 and increases to 8.4 mm yr^{-1} in 2100. The high scenario starts with a rate of 7.9 mm yr^{-1} in 2021 and accelerates to a rate of 12.3 mm yr^{-1} by 2100. Since our input datasets were collected over 2017-2021, we began our simulations in 2020.

Determining C vulnerability to sea-level rise was straight forward and combined published spatially explicit aboveground biomass values for DDNWR (57-59 Mg C/ha) and a belowground biomass value for basin mangroves of 273 ± 26 Mg C/ha (Peneva-Reed and others, 2021). Here-in, we assume that submerged mangroves eventually lead to loss of C but concede that not all C is lost when mangroves are submerged, especially if labile carbon is transported to the estuary as alkalinity (Maher and others, 2018). WARMER-Mangroves was validated using the average SEC rate from our four-year SET record at DDNWR. A model spin-up scheme was used during calibration by using observed deviations in mean sea level from the Ft. Myers, Florida, gauge (station: 8725520), rather than a 2nd order polynomial fit to mean sea level (or 58-years for this station). Initial elevations of each SET were determined by subtracting the mean SEC rate from current absolute soil surface elevation (measured by differential levelling; Buffington and others, 2021).

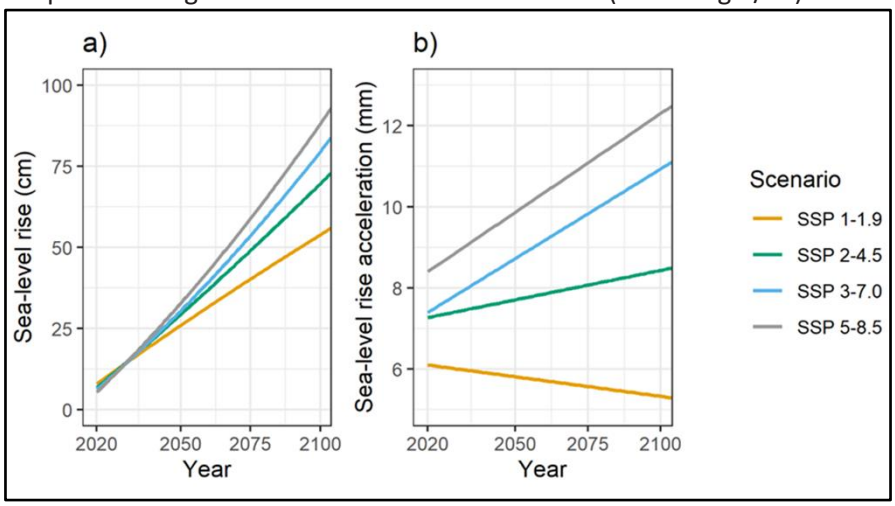

Figure 5. Sea-level rise projections used for Sanibel Island, Florida as incorporated into WARMER simulations. The total level of sea-level rise projected (**a**) and the rate of acceleration (**b**) through 2100.

Results

Experimental Loading of Nutrients on Soil Surface Elevation Change

Annual rates of SEC were positive for all treatments, indicating a gain in soil surface elevation. Nutrient x zone interactions were also evident ($p > 0.05$), with basin mangroves at DDNWR losing elevation with +P treatment and fringe mangroves gaining elevation with +P treatment (**fig. 6**). Conversely, +N treatments had no influence on SEC. Furthermore, SEC differed between mangrove zones regardless of treatment ($F_{1,769} = 70.381$; $p < 0.001$). SEC in basin forests ranged from 4.21 ± 0.58 mm/year to 6.39 ± 0.59 mm/year versus 0.67 ± 0.59 mm/year to 2.13 ± 0.61 mm/year for fringe mangroves (**Table 1**).

High rates of erosion on the fringe removed all MHs within 9 months of deployment; basin MHs remained. Surface accretion in the basin zone ranged from 1.2 ± 0.7 mm/year to 2.2 ± 0.7 mm/year and slope change over time was significantly different from zero, indicating a positive contribution of mineral sedimentation to soil volume. In contrast to SEC, rates of surface accretion did not differ significantly by nutrient treatment versus control plots ($F_{3,4} = 0.72$, $p = 0.59$) (**Table 1**). Shallow subsidence of the basin zone ranged from 2.49 mm/year to 5.16 mm/year, indicating a contribution by belowground processes, such as root decomposition, to SEC even as surface elevations increased. Basin mangroves at DDNWR had an elevation surplus relative to SLR of 0.8 to 3.0 mm/year while fringe mangroves posited an elevation deficit of -1.2 to -2.7 mm/year (**Table 1**).

Table 1. Elevation change, surface accretion, subsurface change, and elevation surplus/deficit. Relative Sea Level Trend (RSLR) for Fort Myers, Florida of 3.37 mm/year was determined from NOAA Station # 8725520. Subsurface change was calculated as the difference between elevation change and accretion. Elevation surplus/deficit was calculated as the difference between measured elevation change and RSLR. All values are annual rates ± 1 SE, in units of mm/year (from Conrad, 2022).

Site	Treatment	Surface elevation change	Surface accretion	Subsurface change	Elevation surplus/deficit
Fringe	Control	0.67 ± 0.59	---	---	-2.70
Fringe	Nitrogen	1.01 ± 0.59	---	---	-2.36
Fringe	Phosphorus	2.13 ± 0.61	---	---	-1.24
Basin	Control	6.39 ± 0.59	1.23 ± 0.65	5.16	3.02
Basin	Nitrogen	5.83 ± 0.58	2.18 ± 0.65	3.65	2.46
Basin	Phosphorus	4.21 ± 0.58	1.72 ± 0.68	2.49	0.84

SEC trends for basin mangroves of DDNWR compared well to 50-year soil accretion trends, but differentiated slightly from 100-year trends in being higher (**fig. 6**). However, the techniques being compared are biased by time scale, such that 100-year trends are often lower than 3-year trends by the different processes included in ^{210}Pb versus SET measurement, respectively.

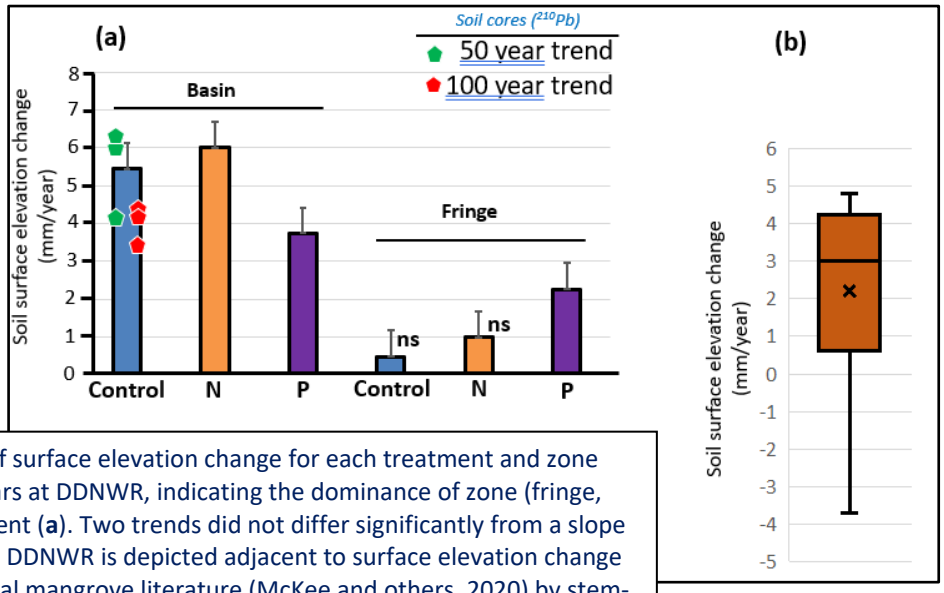

Figure 6. Comparison of surface elevation change for each treatment and zone combination after 4 years at DDNWR, indicating the dominance of zone (fringe, basin) vs. nutrient treatment (**a**). Two trends did not differ significantly from a slope of zero. Comparison from DDNWR is depicted adjacent to surface elevation change rates reported by the global mangrove literature (McKee and others, 2020) by stem-and-leaf plot (non-normal data) (**b**), aligned vertically to the *y*-axis of (a). ^{210}Pb data are as reported by Peneva-Reed and others (2021) and available only for Basin mangroves.

Exchange of CO_2 from Mangrove Soils and Pneumatophores

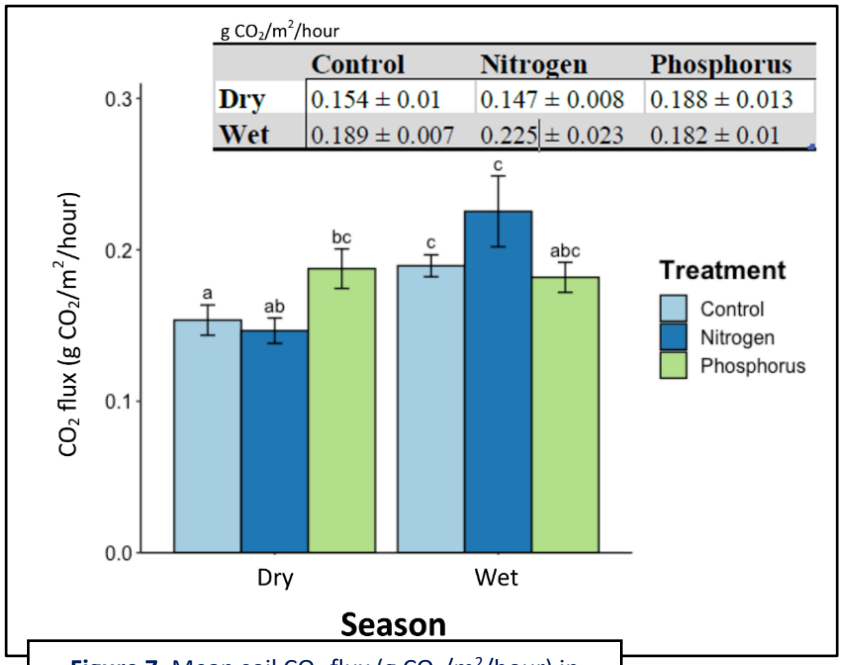

Figure 7. Mean soil CO_2 flux (g CO_2/m^2/hour) in response to experimental nutrient loading and season. Error bars represent ± 1 SE. Bars with the same letter are not significantly different at alpha = 0.05 (from Faron, 2021).

Soil CO_2 flux differed between seasons ($F_{1,60}$ = 29.235, p < 0.001), by sampling day within each season ($F_{2,60}$ = 10.607, p < 0.001), and among treatments (+N, +P) within each season ($F_{2,60}$ = 7.568, p = 0.001). Soil flux from the control and nitrogen (+N) treatments were both significantly greater in the wet season compared to the dry season (p < 0.05). Soil flux increased in the wet season compared to the dry season for the control (23%) and +N treatments (53%), suggesting a higher sensitivity of soil microbes to +N fertilizer compared to phosphorus (+P) fertilizer during the wet season. However, during the dry season, soil CO_2 flux from the +P treatment was significantly greater than the control (p = 0.045) and stimulated the greatest soil CO_2 flux rate across all treatments in the dry season (**fig. 7**). This differs from the wet season results where the +N treatment produced the greatest soil CO_2 flux, demonstrating a shift in nutrient limitation between seasons.

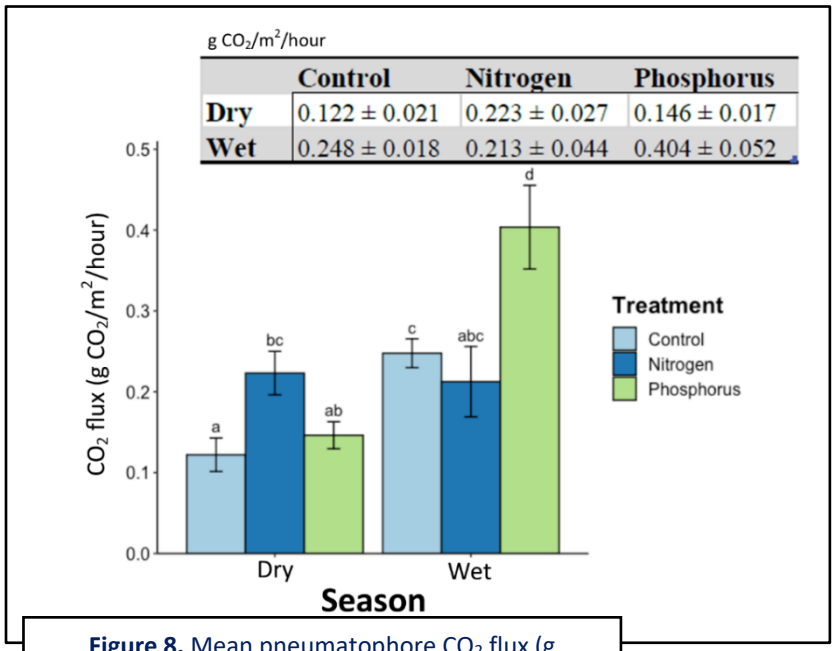

Figure 8. Mean pneumatophore CO_2 flux (g CO_2/m^2/hour) in response to experimental nutrient loading and season. Error bars represent ± 1 SE. Bars with the same letter are not significantly different at alpha = 0.05 (from Faron, 2021).

Likewise, pneumatophore flux also differed between seasons ($F_{1,67}$ = 54.736, p < 0.001), by sampling day within each season ($F_{2,67}$ = 8.8345, p < 0.001), and among treatments within each season ($F_{2,67}$ = 14.001, p < 0.001). Pneumatophore CO_2 flux from the control and +P treatments were both significantly greater in the wet season compared to the dry season (p < 0.05), increasing in the wet season compared to the dry season for the control (103%) and +P treatments (177%; **fig. 8**). Increased

pneumatophore CO_2 flux from the control treatment during the wet season was more than 4 times greater than the increase observed for the control treatment (23%). Furthermore, +P treatment differed from both the control (p = 0.003) and +N (p = 0.004) with greatest increases in the wet season (**fig. 8**).

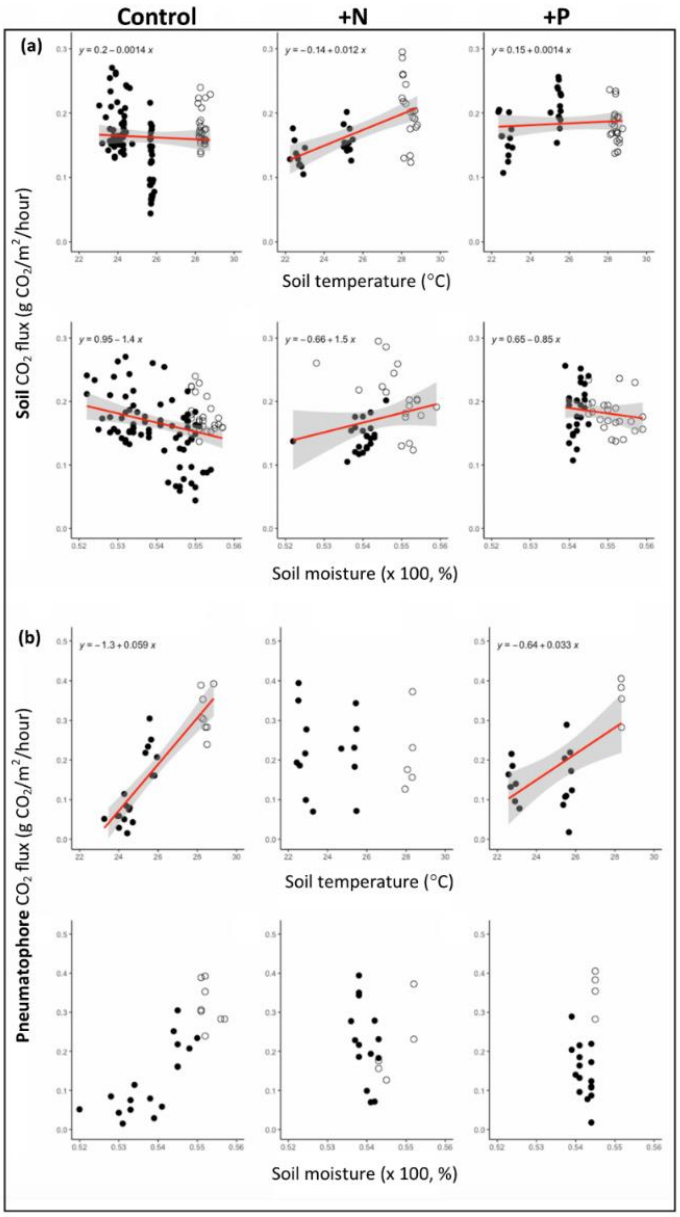

Figure 9. Relationships among soil temperature (°C), soil moisture (%), and soil CO_2 flux (g CO_2/m^2/hour) (**a**), and relationships among soil temperature (°C), soil moisture (%), and pneumatophore CO_2 flux (g CO_2/m^2/hour) (**b**) in control, nitrogen (+N) and phosphorus (+P) treatments, including 95% confidence intervals for prediction (from Faron, 2021).

During the dry season, pneumatophore flux from the +N treatment was significantly greater than the control (p = 0.003). This differs from the wet season and perhaps explains a shift in nutrient limitation between seasons for soil microbes and live plant tissue. Furthermore, the pneumatophore flux in the +N treatment did not differ between seasons and increased by only 5% during the dry season (**fig. 8**). The +P treatment produced a pneumatophore flux response more than 20-fold that of the +N treatment between seasons, suggesting a higher sensitivity of live roots to +P.

As soil temperature increased, soil CO_2 flux rates tended to increase (**fig. 9a**), especially for +N treatments. Likewise, as soil moisture content increased, soil flux rates decreased for control and +P but increased for +N (**fig. 9a**), which may explain why soil CO_2 fluxes were higher in +N treatments during the wet season. Soil temperature and moisture were positively correlated across all treatments ($0.64 \leq r \leq 0.80$; $p < 0.001$).

In contrast to soil CO_2 fluxes, as soil temperature increased, pneumatophore fluxes increased for control and +P treatments but not for +N (**fig. 9b**). These wet/dry season responses were an important distinction in driving understory CO_2 flux in DDNWR mangroves. Even though means among discrete treatments did not differ consistently across wet and dry seasons, the warming of the soil drove greatest soil and pneumatophore fluxes once phosphorus was added. That said, control and +P treatments had proportionately greater CO_2 fluxes from pneumatophore structures per unit increase in soil temperature than for soil CO_2 flux. Soil moisture had no influence on pneumatophore CO_2 fluxes.

Sap flow

The DDNWR sap flow dataset was substantially large and included over 6500 tree-days during two wet season (2019, 2020) and one dry season periods (**Table 2**). Despite many measurements, we found no effect of treatment (control, +N, +P) on average daily maximum rates of sap flow in either *A. germinans* or *R. mangle* at a radial sapwood depth of 5 mm (**fig. 10**); however, sap flow at 5 mm was only 62% and 53% of sap flow at 15 mm, respectively. Additionally, there were no treatment differences for either *A. germinans* or *R. mangle* at a radial sapwood depth of 15 mm. Despite this, for maximum flows during wet season periods, sap flow at 5 mm was higher across both species ($F_{1,1}$ = 6.886, p = 0.011) with a least square means of 18.2 g $H_2O/m^2/s$. Wet season versus dry season differences were somewhat confounding, but important in driving water usage by these mangroves with transition from significant and non-significant influences across treatment combinations. Also, the two species differed in how they used water at specific points into the sapwood. For example, at a radial of 15 mm, *A. germinans* registered significantly higher ($F_{1,1}$ = 7.917, p = 0.007) overall average daily maximum sap flow rates across all seasons, with a least square mean of 41.71 g $H_2O/m^2/s$ compared to *R. mangle* (least square mean, 33.73 g $H_2O/m^2/s$).

In contrast, when sap flow at 5 mm and 15 mm radial depths were integrated by sapwood area into calculations of outer sapwood water use (L H_2O/day), *R. mangle* trees used less water in +N and +P treatments than in control treatments (**fig. 11**). This species trend reversed as additional depths of integration (at 50, 70, 90 mm) were added, expanding sapwood areas to incorporate a 90 mm sapwood radius (**Table 3**).

Table 2. Number of sap flow study trees used by mangrove species (black, *Avicennia germinans*; red, *Rhizophora mangle*), treatment (control, nitrogen (+N), phosphorus (+P)) and number of sample days (from Miller, 2022).

	Growing Season 2019 (02 May - 15 Aug 2019)			Dry Season 2020 (03 Feb - 23 Mar 2020)			Growing Season 2020 (06 Jun - 05 Oct 2020)		
Treatment	Red Mangrove	Black Mangrove	# Days	Red Mangrove	Black Mangrove	# Days	Red Mangrove	Black Mangrove	# Days
Nitrogen	4	4	92	2[b]	4	49	3[b]	4	120
Phosphorus	4	4	45[a]	2	4	49	3	5	123
Control	6[c]	6[d]	104	6[d]	6[c]	49	6[d]	6[c]	122

[a]Data download error caused loss of data from 29 June– 12 August 2019.
[b]Includes (1) tree probed outside of treatment/control plots.
[c]Includes (2) trees probed outside of treatment/control plots.
[d]Includes (3) trees probed outside of treatment/control plots.

Stand Water Use

Hurricane damage legacies existed for DDNWR mangroves even after > 15 years post Hurricane Charley. In fact, all mangrove stands surveyed were in some phase of recovery. Average *S* among the 85 basin forest plots was 594.3 ± 21.5 mm H_2O/year (range, 226–1181 mm H_2O/year). Smaller plot sizes created greater variability in estimation of *S*, indicating that small forest structural shifts among species and

Table 3. Maximum wet season sapflow (g $H_2O/m^2/s$) at a radial sapwood depth of 5, 15, 50, 70, and 90 mm by mangrove species, and modeling attenuation coefficients relative to 15 mm flows (Miller, 2022).

	Sapflow (g $H_2O/m^2/s$)					Proportional attenuation by depth				
Radial sapwood depth (mm)	5	15	50	70	90	5	15	50	70	90
R. mangle										
All treatments	24.87	46.09	20.62	29.22	14.12	0.539	1.000	0.447	0.634	0.306
+N	17.83	42.93	40.99		3.56	0.415	1.000	0.955		0.083
+P	31.67	47.25				0.670	1.000			
Control	24.96	47.10	13.83	29.22	17.65	0.530	1.000	0.294	0.620	0.375
A. germinans										
All treatments	32.57	53.26	24.92	15.28	16.05	0.612	1.000	0.468	0.287	0.301
+N	27.39	57.17	17.24	10.96	22.14	0.479	1.000	0.302	0.192	0.387
+P	32.70	47.32	30.72	11.11	13.55	0.691	1.000	0.649	0.235	0.286
Control	32.31	52.14	28.68	19.49	8.87	0.620	1.000	0.550	0.374	0.170

size classes affect this hydrologic metric. Likewise, average *S* among the 43 fringe forest plots modelled was 521.0 ± 27.2 mm H_2O/year (range, 158–1046 mm H_2O/year). Of note are the two lowest values of 226 mm H_2O/year for basin and 158 mm H_2O/year for fringe. These values were not outliers, as several sites were sparsely populated with trees.

Stand water use was not influenced strongly by the +N treatment but was influenced by +P; even slight changes in *S* among treatment combinations scale in ways to suggest important metabolic consequences of the +P treatment. *S* becomes 571.1 ± 21.3 mm H_2O/year for +N and 615.7 ± 20.3 mm H_2O/year for +P basin mangroves, and points to a notable increase in water use when additional phosphorus is delivered. Detecting such a difference of ~45 mm H_2O/year would require well over 25 estimates of *S* (Krauss and others, 2015), and our experimental design incorporated an appropriate sampling intensity. A similar increase in *S* in +P treatments occurred in fringe mangroves, where *S* becomes 603.2 ± 32.0 mm H_2O/year. Likewise, +N treatment had no influence on *S* in fringe mangroves

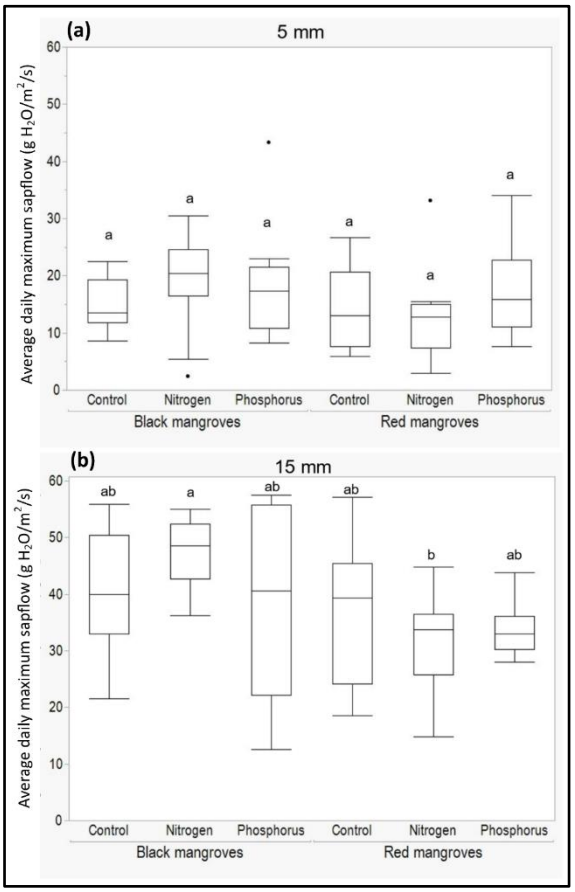

Figure 10. Average daily maximum sap flow rates (g $H_2O/m^2/s$) measured at radial depths of 5 mm (**a**) and 15 mm (**b**) into the sapwood of trees by mangrove species (black, *Avicennia germinans*; red, *Rhizophora mangle*) by treatment (control, +N, +P). Different letters represent statistically significant differences as determined by a Tukey's HSD test at alpha = 0.05 (from Miller, 2022).

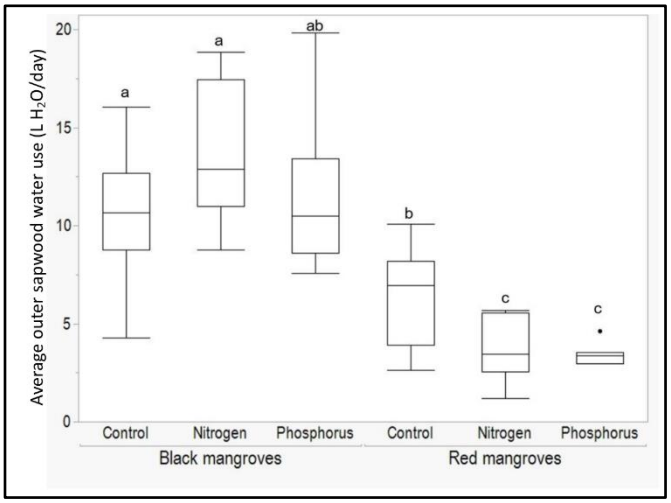

Figure 11. Daily water use (L H_2O/day) by the outer sapwood (to a radial depth of 0-20 mm) of mangrove trees (black, *Avicennia germinans*; red, *Rhizophora mangle*) by treatment (control, +N, +P). Different letters represent statistically significant differences as determined by a Tukey's HSD test at alpha = 0.05 (from Miller, 2022).

(**Table 1-2**). Overall, *S* remained static for basin and fringe +N treatments versus controls, was stimulated by 3.6% in +P-fertilized basin mangroves versus controls, and was stimulated by 15.8% in +P-fertilized fringe mangroves versus controls. By individual species, the majority of increases in *S* under enhanced phosphorus loading was associated with *R. mangle* trees (**fig. 12**); greater individual tree water usage was compounded by larger *R. mangle* trees in fringe environments than in basin environments.

Determining Ecosystem Carbon Fluxes and Vulnerability

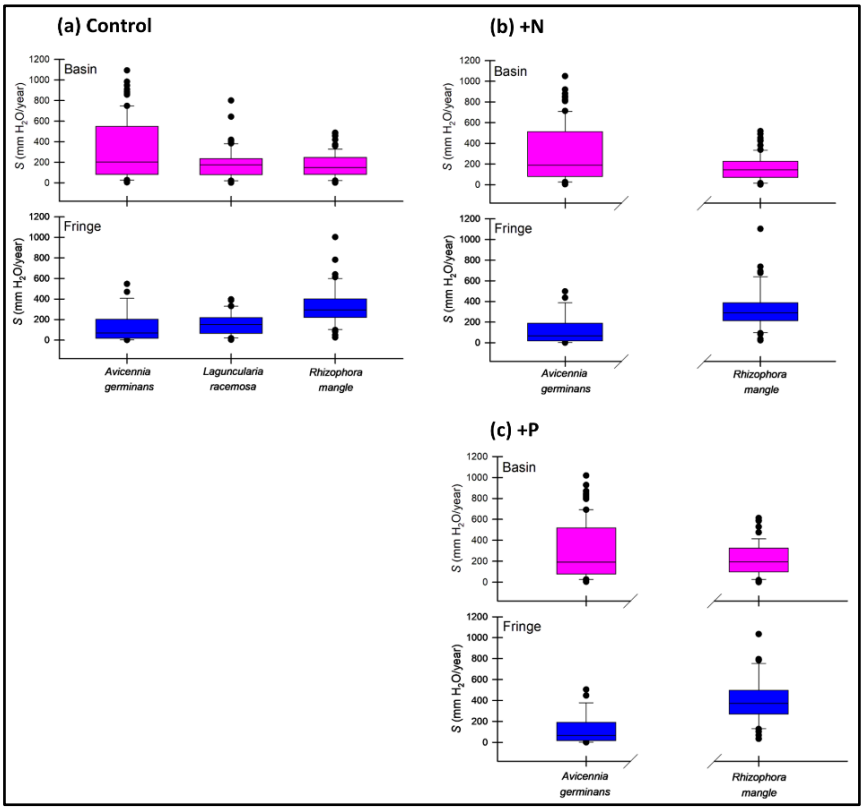

Figure 12. Modeled rates of stand water use (*S*) by zone (basin, fringe), species, and treatment for mangroves growing across 128 study plots at DDNWR.

In order to determine the influence of +N-treatment and +P-treatment on C fluxes, we established a baseline C budget using data from our experimental controls. First, CO_2 fluxes from the soil and pneumatophores were modelled on daily timesteps over the two study years (**fig. 13**). Using these regressions versus weather station air/soil temperature data, annual fluxes of CO_2 from soils and pneumatophores summed to 457.1 g C/m^2/year for control, with 30.4% greater CO_2 flux volume from pneumatophores versus soils. Soil and pneumatophore CO_2 fluxes ranged from 0.8 to 1.4 g C/m^2/day.

Second, GPP was estimated from *S* on an hourly time step using WUE_i, stratified by the functional sapwood area distribution of mangrove species on each of the 128 plots. Annual uptake of CO_2 by GPP averaged 871.9 g C/m^2/year for control, ranging from 0.2 to 3.7 g C/m^2/day. Using Equation [3], annual fluxes of CO_2 as NEE_c averaged -414.9 6 g C/m^2/year, ranging from 0.7 to -2.5 g C/m^2/day (negative values denote uptake of C) (**fig. 14**). Third, we note that C_B averages 134.7 g C/m^2/year (Peneva-Reed and others, 2021), but because we only dated three cores successfully, we explored the full range of possible C_B options during C budget development using average (134.7 g C/m^2/year), low (69.4 g C/m^2/year), and high (180.0 g C/m^2/year) C_B values from the three cores. We determine that surface sediment C accumulation for control plots average 17.9 g C/m^2/year, ranging from 0 g C/m^2/year for erosive fringe environments to 35.7 g C/m^2/year for basin environments. Finally, in applying Equation [4], lateral carbon flux ($C_{E/I}$) is estimated to be approximately 262.3 g/m^2/year (control plot values), exported from the mangroves. This value ranges from 220 to 328 g C/m^2/year depending on whether we used average, low, or high C_B values.

These data were then scaled to the entire mangrove area at DDNWR, or 1112 ± 116 ha (Peneva-Reed and others, 2021), and converted to units of Gg C to develop a total mass balance C budget for DDNWR's mangroves (**fig. 15a**). We then applied the same procedures to N-fertilized and P-fertilized plots as we did for controls, thereby simulating what influence additional nutrient loading might have on mangrove C mass balances (**fig. 15b,c**). From these simulations, mangroves at DDNWR experienced little alteration in C budgeting under +N scenarios relative to control scenarios. Importantly, +N-treatment had limited influence on how the ecosystems used water through vegetation, and therefore additional nitrogen would also not be expected to stimulate GPP in significant ways. Despite disparate N:P ratios at DDNWR, this system is likely operating at its maximum capacity for nitrogen uptake already. Furthermore, species distributions of *A. germinans* and *R. mangle* between basin and fringe environments also did not change the balance of *S* significantly until +P was applied. In fact, too

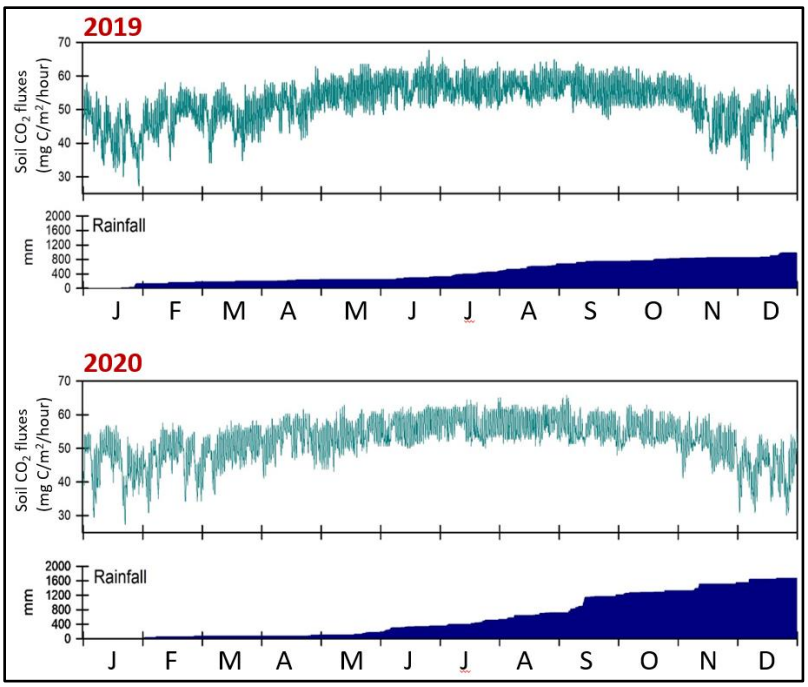

Figure 13. Modeled soil carbon fluxes from CO_2 exchange (mg C/m^2/hour) for DDNWR control plots (without fertilization) for two years, and cumulative rainfall (mm H_2O). Data represent control plots.

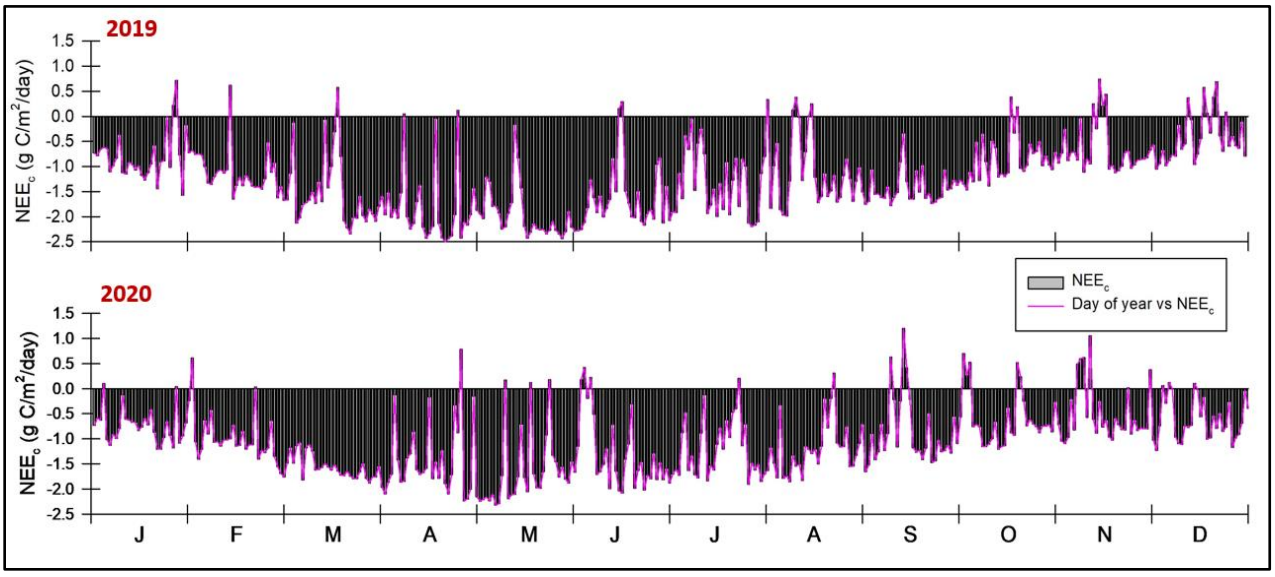

Figure 14. Net ecosystem exchange of carbon (NEE_c) from the mangroves of DDNWR for two study years (2019, 2020). Data represent control plots.

much nitrogen may be serving as a constraint to GPP and soil CO_2 flux, and therefore +N is projected to decrease lateral fluxes of C into estuarine waters by a small amount, or 0.3 GgC, which is likely to be insignificant (**fig. 15b**).

In contrast, the +P treatment was more impactful to DDNWR's mangrove C budget, stimulating greater stand water use, higher GPP, higher C uptake as NEE_c, and a greater projected lateral export of carbon to estuarine waters by 1.2 GgC annually versus controls (**Fig. 15c**). Greater water usage by *R. mangle* (by 28% vs. control) with +P-loading was partly responsible. An increase in lateral C fluxes with additional +P-loading has the potential to further stimulate aquatic N and P mineralization from organic matter breakdown and contribute further to estuarine eutrophication while causing a more expedient deterioration of the mangroves regardless of future sea-level rise scenarios realized.

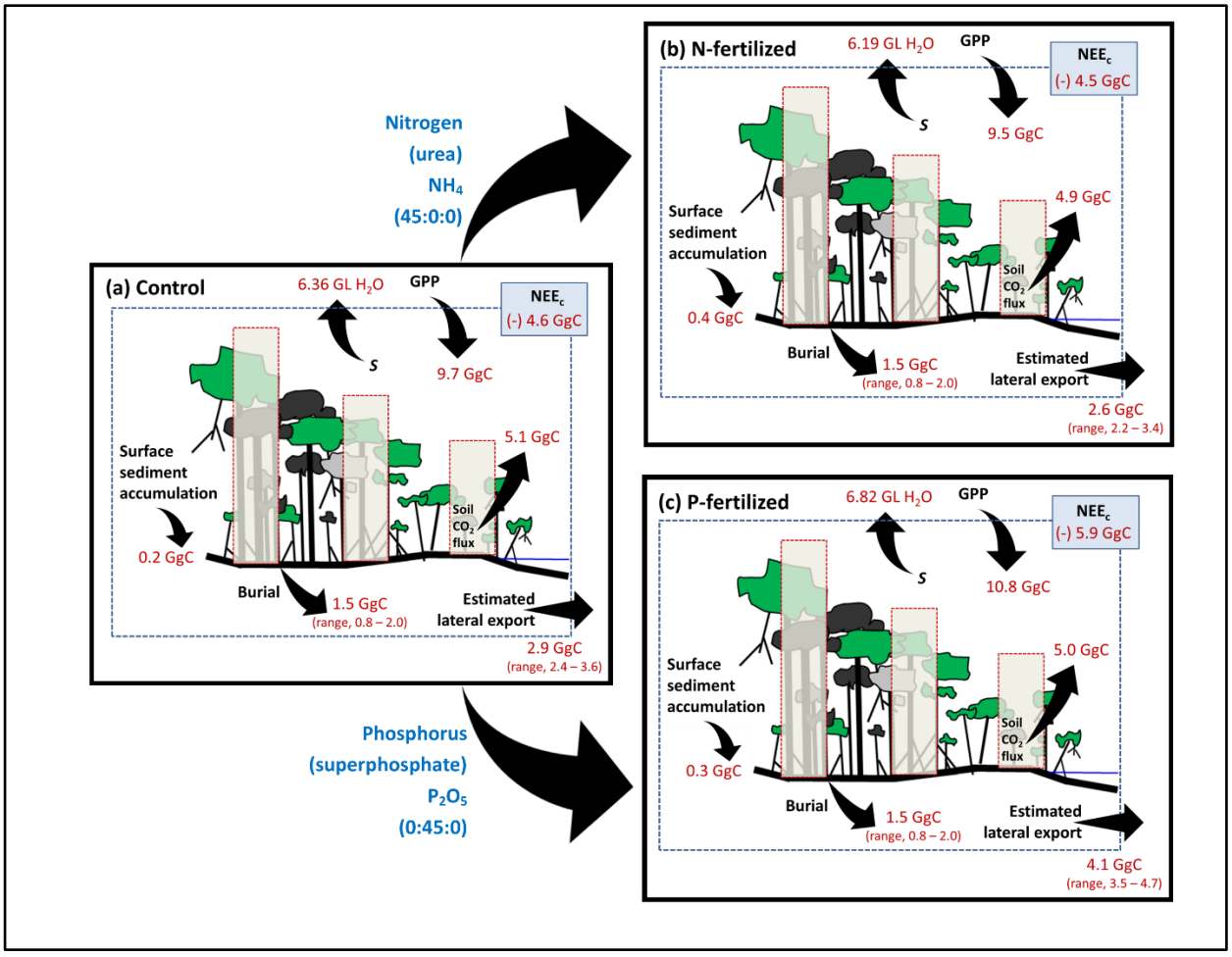

Figure 15. Carbon budget for all 1112 ha of mangroves at DDNWR, reported for control (**a**), +N-fertilized (**b**), and +P-fertilized (**c**) scenarios. Sites were fertilized twice annually for three years using granular, slow-release fertilizers applied into soils at 2 × 2 m grid spacing. Efficacy of this procedure as applied to an intertidal environment was confirmed (Miller, 2022). GPP = gross primary productivity; NEE_c = net ecosystem exchange of carbon; *S* = stand water use.

Modelling of Sea-level Rise and Carbon Vulnerability

Over the historic spin-up period used for model calibration, the model projected an average accretion rate of 5.3 ± 0.4 mm yr^{-1}, which was not significantly different than the 50-year accretion rates of 5.7 ± 0.11 mm yr^{-1} as determined from ^{210}Pb dating. The mean rate of accretion from the SETs was 6.4 ± 0.8 mm yr^{-1} over four years (Conrad, 2022), while the model projected accretion of 4.9 ± 0.5 mm yr^{-1} using water level data from a nearby NOAA gauge to force the model.

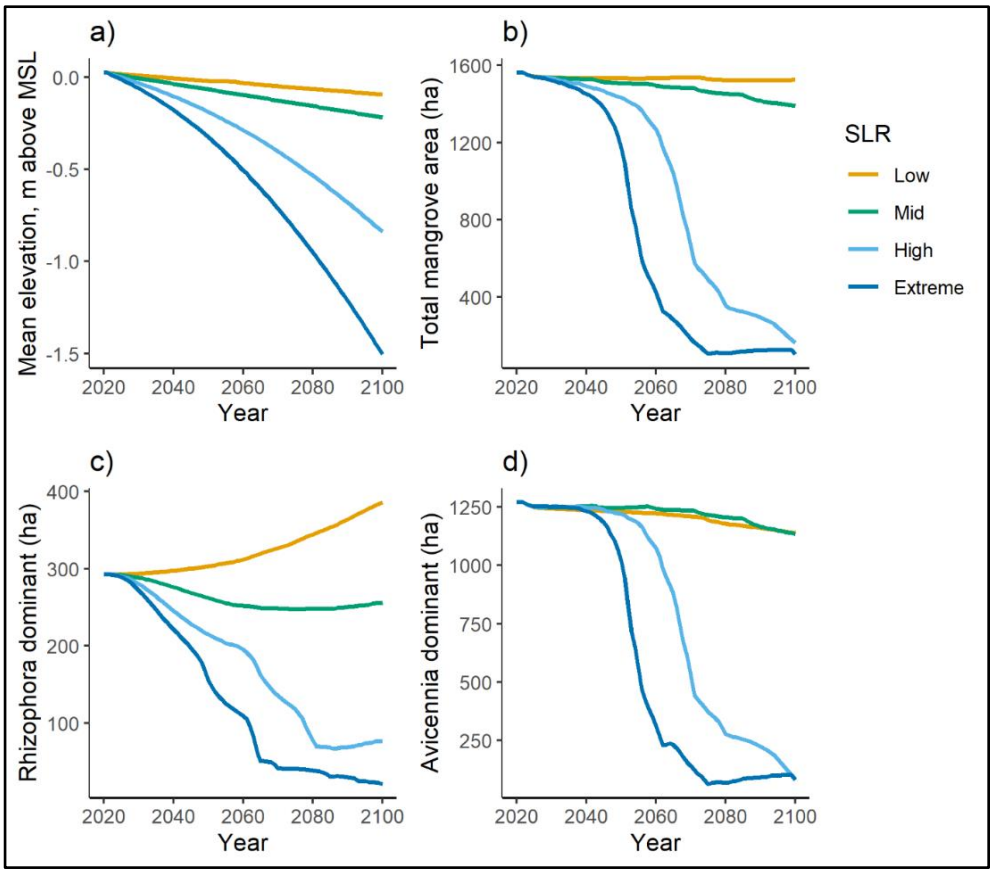

Figure 16. Projections of elevation and mangrove cover under four sea-level rise (SLR) scenarios across Ding Darling National Wildlife Refuge. Mean elevation of the study domain relative to mean sea level (MSL; **a**). Projected area (hectares) of mangrove across the study domain (**b**), and area that is dominated by *Rhizophora* (**c**) and *Avicennia* (**d**) mangroves.

If sea-level rise at Sanibel Island would track up to even double historic rates, changes in mangrove forest area through 2100 would be modest. Simulations of the lowest sea-level rise rate in the IPCC AR6 report through 2100 indicate small decreases in mangrove area of approximately 89.1 ha compared with the current total area of 866 ha (or -10.3%) (**fig. 16**). More extensive submergence is projected to occur with an inflection of sea-level rise to 70 cm by 2100, with an estimated 266.6 ha lost by 2100 (-30.8%). Submergence was projected to be much more rapid and extensive under the medium sea-level rise scenario of 80 cm by 2100, with 666.1 ha lost (76.9%). With the high scenario of 88 cm by 2100, nearly all of the mangroves within our domain are projected to be submerged, with an estimated 847.8 ha lost (97.9%) (**fig. 17**). However, it is important to note that submergence would not immediately beget loss; there is a potential lag between the two that would be moderated by estuarine fetch, wind aspect, waves, and storms. It is also important to note that model domain for WARMER-Mangroves was smaller than the total mangrove area mapped by Peneva-Reed and others (2021) because smaller mangrove patches and landward edge habitat with limited elevation data could not be included with confidence in WARMER-Mangroves.

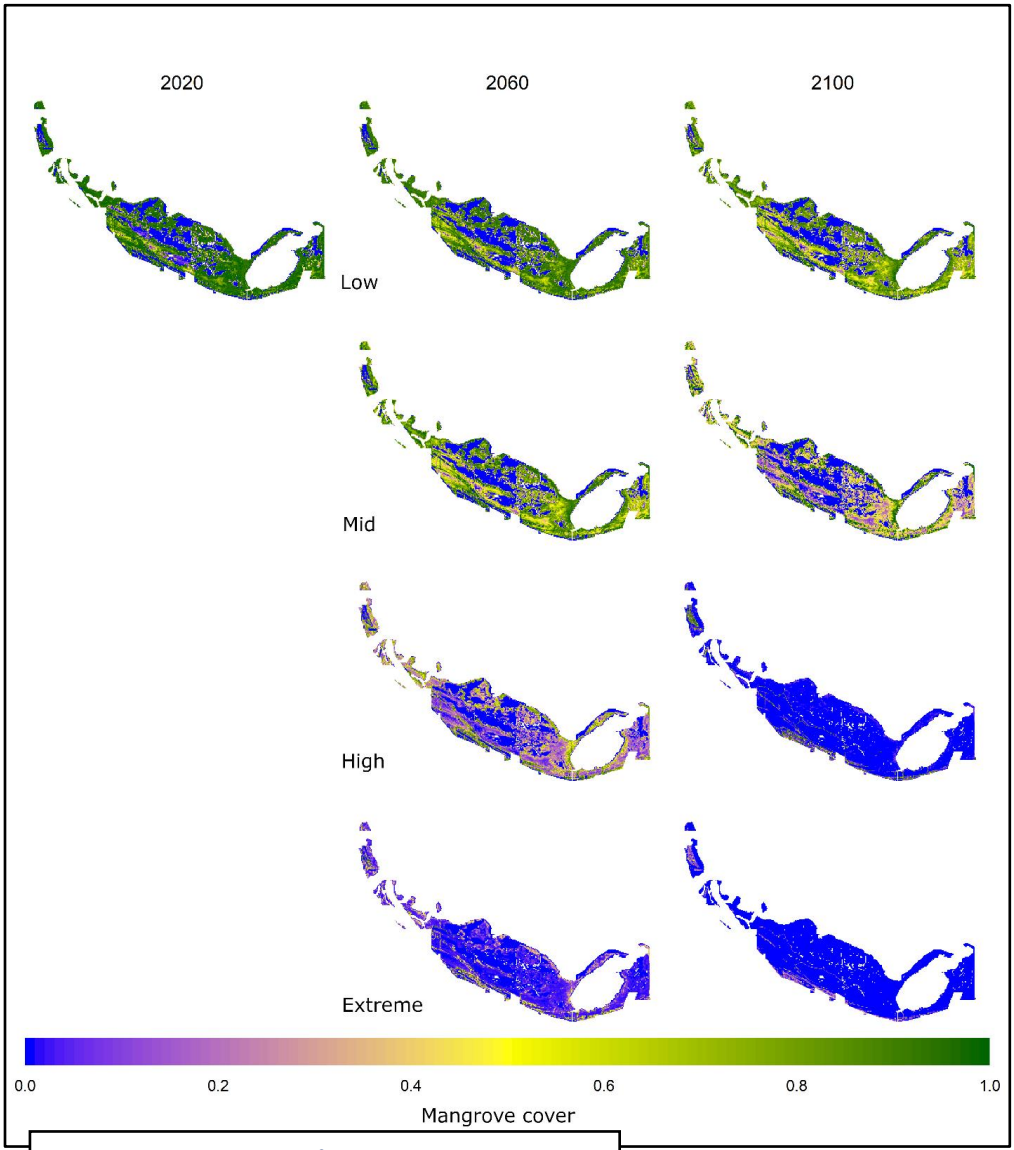

Figure 17. Projections of mangrove cover in 2060 and 2100 across Ding Darling National Wildlife refuge under four sea-level rise scenarios.

Under low sea-level rise, aboveground biomass carbon was projected to decrease by 5.2 Gg C, while under medium, high, and extreme sea-level rise scenarios, aboveground biomass carbon of Sanibel Island's mangroves was projected to be reduced by 15.5, 38.6, and 49.2 Gg C, respectively. For belowground biomass, the model projected a decrease of 24.3, 72.8, 181.8, and 231.5 Gg C by 2100 under low, medium, high, and extreme sea-level rise (**fig. 18**). These projections assume all carbon is removed from the system upon loss of living mangroves and represent an endmember projection since the fate of carbon upon transition to an unvegetated state is not well known. The low sea-level rise scenario is compatible with our C budget developed for the control scenario (**Fig. 15a**); NEE_c of -4.6 GgC/year and low lateral fluxes (~2.9 GgC/year) would build C over time as submergence, soil cohort transfers, and unaccounted respiration are included.

Synthesis

We found little evidence that the mangroves of DDNWR were experiencing nutrient limitation of any kind. We further conclude that additional loading of P is likely to become increasingly detrimental to the metabolic processes of DDNWR's mangroves, increase their susceptibility to rising seas through

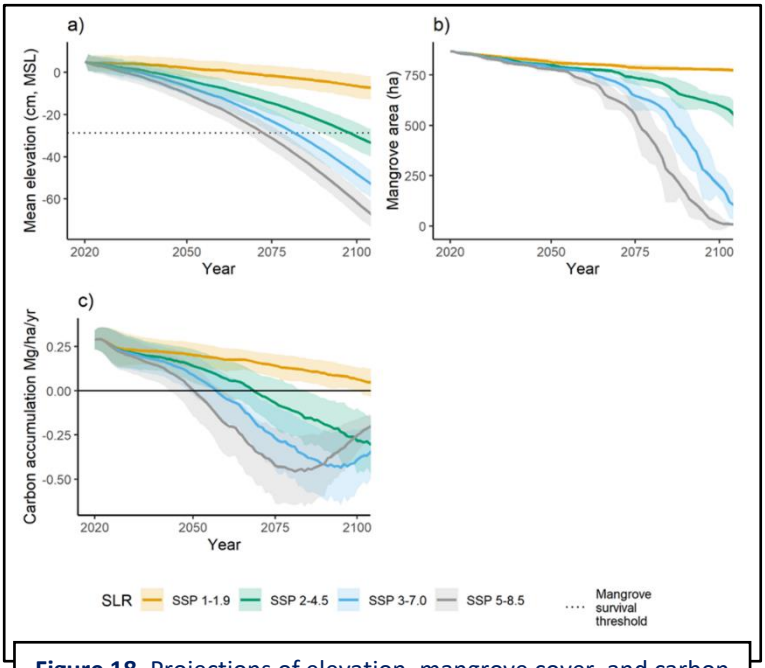

Figure 18. Projections of elevation, mangrove cover, and carbon accumulation rate under five sea-level rise (SLR) scenarios across Ding Darling National Wildlife Refuge. Mean elevation of the study domain relative to mean sea level (MSL) and the assumed lower limit of mangrove survival (**a**). Projected area (hectares) of mangrove across the study domain (**b**), and carbon accumulation rate (Mg/ha/year; **c**).

surface elevation losses, and provide more C export to promote mineralization and additional estuarine eutrophication. Indeed, DDNWR's mangroves appear to be at the physiological limit of growth with the N and P already present in soils and will not likely have sink capacity for additional nutrients. Soil surface elevation was reduced by additional P (but not +N) over the three study years, and when additional +P and +N treatment differences were evident for soil and pneumatophore CO_2 fluxes, sap flow, or stand water use, differences were generally nuanced by seasonality, hydroperiod factors, emergent individual tree scaling, or in how data were summed or analyzed. Greater differences in soil surface elevation could have manifested over a longer study duration. Except for soil surface elevation change, no differences in +N or +P treatments would be considered extreme; at least not until C mass balances were evaluated. Such moderate responses can be expected in an estuary that is already eutrophic (DeGrove, 1981; Bricker and others, 1999; Lapointe and Bedford, 2007); degradation by small degrees as demonstrated in the Florida Everglades (Douglas, 1997) despite healthy regeneration (**fig. 19**).

The current nutrient state of DDNWR's mangroves may already be driving deterioration of the system in subtle and somewhat inconsistent ways. Subtle degradation is common in mangroves, as their stress tolerance serves as a barrier to identifying pressing issues that might be ameliorated by implementation of management action (Lewis and others, 2016). Basin mangroves demonstrated very strong ability to build soil surface elevations in the presence of rising sea levels despite DDNWR's current state of P eutrophication. This capacity was commensurate with nearby basin mangroves in Southwest Florida with far lower soil nutrient concentrations

Figure 19. Healthy, regenerating fringe-to-basin mangrove forest transition at Ding Darling NWR (Photograph by Ken W. Krauss, U.S. Geological Survey).

(Cahoon and Lynch, 1997); however, some of the capacity to build soil surface elevations at DDNWR was related to organic matter surface deposition of litter, branches, and wood flakes from deteriorating canopies given rise to vertically expanding, but unconsolidated soils. Soil surface increment in P-limited environments is stimulated through root volume expansion (McKee and others, 2007), the capacity for which remained undocumented at DDNWR. Root C biomass production ranged from ~131 to 244 g C/m^2/year but was unaffected by +N and +P fertilization (Conrad, 2022), suggesting that antecedent soil nutritional state might have been the primary difference in projected versus actual response for DDNWR's mangroves.

Metabolically, respiration from soil and belowground root structures was high at DDNWR (vs. Lovelock, 2008; Lovelock and others, 2014b; Hien and others, 2018), especially in the wet season when river water exchange was more direct. Additional N influenced soil respiration rates more in the wet season and additional P influenced soil respiration rates more in the dry season, suggesting a potentially critical shift in bioavailable forms of N and P seasonally that persist because microbial and plant tissue N and P responses are near saturation. For example, P stimulation of pneumatophore CO_2 fluxes was highest in the wet season, in contrast to soil respiration. Thus, soils and roots are responding differently. It is possible that some seasonal N limitation occurs as P is depleted from root structures, and increased P loading from the Caloosahatchee River could eliminate further P uptake and devalue the role of DDNWR's mangroves in nutrient retention for enhanced water quality remediation of the estuary.

Since new basal area growth stimulated by nutrient addition would be reflected in our shallowest sap flow measurements at 5 mm, and because N and P limitation impacts water uptake and transport in plants (Carvajal and others, 1996; Clarkson and others, 2000), we expected to see the largest increase in sap flow rates with +N treatment and +P treatment at radial sapwood depths of 5 mm. We did not. This is an indication that water transport within the most nutrient-responsive tissue is not likely being limited by nutrients. Based on high soil respiration rates, mineralization of soil N and P pools to become bioavailable for mangrove uptake (if possible) or flux into estuarine waters is also likely. *Avicennia germinans* trees appear to be operating at their eco-physiological maximum with the background nutrient concentrations present at DDNWR, but this might not be the case for *R. mangle*. Furthermore, our knowledge is limited about *Laguncularia racemosa* and whether that species adds to *S* (and GPP) or offsets *S* (and GPP) with +N or +P loading to DDNWR.

Both *A. germinans* and *R. mangle* tree water transport were affected differentially by nutrient addition because of differences in their physiology and the microhabitats they occupy. Phosphorus fertilization altered how *R. mangle* trees used water at deeper sapwood depths such that where this species was more dominant versus *A. germinans* and *L. racemosa*, *S* became concomitantly higher with P fertilization. *Rhizophora mangle* is more dominant along the fringe zone where P is more commonly flushed from soils by tide (Krauss and others, 2006), while *Avicennia germinans* is more widespread in the basin zone and has a very broad adaptation to environmental stressors. Robert and others (2009) found that a congeneric mangrove species, *Avicennia marina*, in Kenya had higher stem vessel density, higher vessel grouping, and smaller vessel diameter than *R. mangle*'s congeneric, *Rhizophora mucronata*. Anatomical differences lead to "safer" water transport systems in *Avicennia* (Krauss and others, 2007); *Rhizophora* is more responsive, as we also discovered at DDNWR. Overall, mangroves are efficient at regulating their water use and, simultaneously, very efficient at CO_2 uptake despite this low water use (Krauss and others, 2022a). Therefore, responses to nutrient enrichment or limitation in mangroves are likely to be conservative in influence, affect water use efficiency at all scales (leaf, plant, stand), and provide a useful approach to estimating environmental influences on GPP.

Fluxes of CO_2 that contribute to forest ecosystem GPP are especially sensitive to fluctuations in air temperature and relative humidity that control diffusion gradients of both water and CO_2 (Baldocchi, 2003; Shoemaker and others, 2022). Our approach, which we consider an "inverse modeling approach," considers atmosphere diffusion gradients for water and the feedback that water limitations impose on

gross CO_2 uptake of the mangrove forest. This gross CO_2 uptake represents all of the C entering the system through vegetation, supplemented by fluvial and tidal C deposition to complete the C budget. Variation in functional sapwood area among trees of the same species and maximum values of J_s used for determining water use potential by size class and species provide a limitation to the inverse modeling approach. The benefit of using inverse modeling versus EC approaches includes, among major cost and staffing requirements for EC, providing an eco-physiological mechanism for determining what experimental manipulations might have on GPP and NEE_c over short time periods from areas small enough to apply experimental treatments.

For DDNWR, an important finding is that additional P loading to Pine Island Sound and its surrounding mangroves may promote greater lateral exports of C in the form of DOC, DIC, and POC, and make the retention of C less likely for the mangroves into the future (**fig. 15**). Reductions of soil surface elevation from Sanibel Island's basin mangroves are also suggestive of soil structural losses. Release of N and P from aquatic mineralization of DOC could contribute to additional eutrophication as the mangroves export more C-based compounds with additional P loading. That stated, inference around this conclusion could be augmented significantly with additional estimates of C_B from DDNWR to include fringe mangroves and landward edge mangrove boundaries of *Conocarpus*. Furthermore, the lag time between stand water use and environmental drivers of water use (for example, *D*) over a daily cycle makes analysis using this approach less useful when comparing among individual days, as GPP response is surmised from *S* and modelled to occur into the night as does water movement. This is an artifact of our inverse modeling approach and suggests that application may need to be averaged across many days, making comparison among weeks, months, or years a more reasonable statistical exercise.

Management Implications

The potential pattern of mangrove loss on the fringe countered by inland migration of mangroves, or transgression, has implications for DDNWR land managers (**fig. 20**). For one, tidal wetlands must have the capacity to build elevations in order to migrate inland; they do not need to build faster than sea-level rise to do this. While there may be limited concern from slow sea level-rise, land managers may work to improve habitat quality and build natural resiliency into the system to push back against modest accelerations in sea-level rise. For the mangroves of DDNWR, regulating P discharge down the Caloosahatchee River is among those options available to achieve the outcomes of inland migration potential, in-situ soil building, and soil P retention for DDNWR's mangroves. Currently, soil P is being sequestered at exceptionally high rates of 36.6 g P/m^2/year in fringe and 96.2 g P/m^2/year in basin

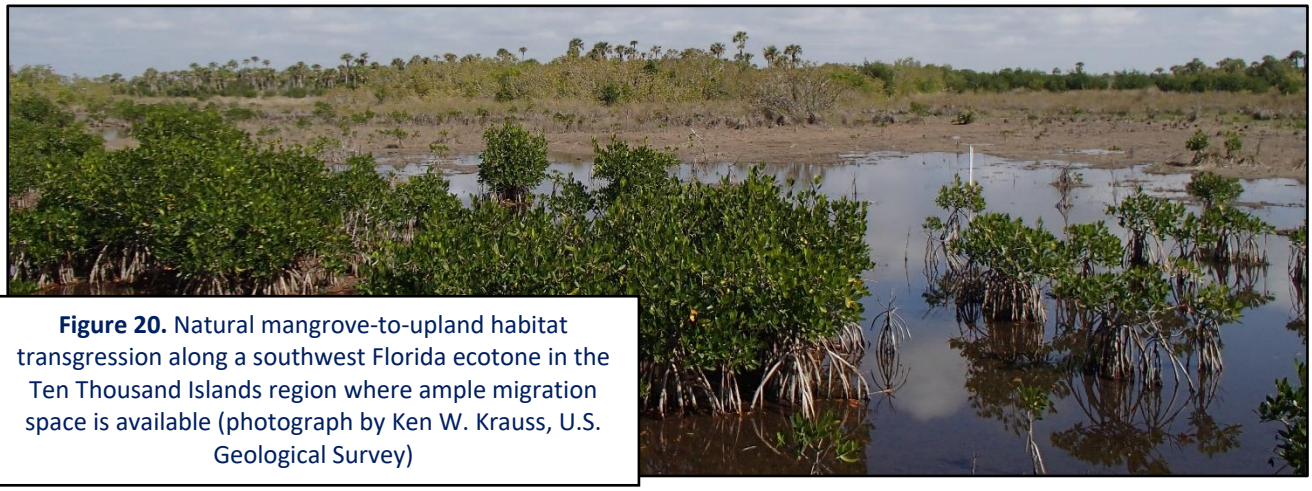

Figure 20. Natural mangrove-to-upland habitat transgression along a southwest Florida ecotone in the Ten Thousand Islands region where ample migration space is available (photograph by Ken W. Krauss, U.S. Geological Survey)

mangroves (procedures outlined by Cormier and others, 2022), representing a substantial increase in average annual accumulation over the last 100 years within Sanibel Island's basin mangroves (1.25 g P/m^2/year; Drexler, 2019). We note here that differences between 3-year and 100-year P accumulation rates are influenced by time-scale bias inherent to the different techniques (Breithaupt and others, 2018). However, mangroves will not be able to take up additional P without significantly altering patterns of surface elevation change or sedimentation, thus limiting further mangrove-facilitated water quality improvement aspirations for Pine Island Sound.

Working with federal, state, local, and tribal partners to improve local water quality conditions in the Caloosahatchee Estuary can serve to facilitate a regeneration of near shore seagrass beds, improved oyster reproduction and reef development, and increased mangrove forest productivity, all of which can contribute to an increase in soil surface elevations. Mangroves have a natural ability to adjust to rising sea levels, if they remain healthy (Krauss and others, 2014). Additionally, managers may work to address the erosive forces in the fringe mangrove zone by reducing impacts from wave energy created from the local boating and fishing communities. Managers may implement "no wake zones" for motorboats near sensitive and exposed fringe zones; erosion was so high in our fringe mangroves that MH layers did not last a week. Managers may also support near shore oyster reef restoration projects that can serve to attenuate wave energy to the mangroves while improving water quality. Lastly, managers can track the rate of transgression with remote sensing technologies and identify barriers to inland migration, then work to remove those barriers such that inland migration can occur. For example, expanding the boundary of DDNWR is one scenario, especially given the extreme damage and taxpayer burden delivered from Hurricane Ian (in 2022). Natural ecosystems are far more resistant to hurricanes than built communities. While none of the management strategies evaluated address the rate of sea-level rise directly, together, management actions may improve the rate of soil surface elevation increment in the fringe zone and extend the life of DDNWR's current mangrove forest distribution.

Opportunities may be available for strategic land acquisitions to prevent development and provide options for DDNWR managers to apply their R-A-D (Resist-Accept-Direct) strategy (Lynch and others, 2022). Without uplands to accommodate mangrove migration, "accept" may be the default strategy, and as we show here, significant mangrove areas may be lost in the future, exacerbated by metabolic stimulation with additional P loading from the Caloosahatchee River. One management consideration to preserve barrier islands for natural protection of estuarine ecosystems and sustain wetland ecosystem services is a building moratorium. This strategy may provide a greater benefit to the region in comparison to the current state.

Data Availability

All raw data collected during these studies are available to the public at ScienceBase.gov and are referenced individually in **Appendix 3**.

Project Deliverables

All project publications, presentations, and seminars are reported in **Appendix 4**.

Acknowledgments

This project was borne from the U.S. Geological Survey's (USGS) Biological Carbon Sequestration Program (or LandCarbon), which was an offshoot of the Congressionally authorized Energy Independence and Security Act (EISA) to link refuge management actions to biological carbon integrity within the Nation's wetlands. This research represents a partnership between the U.S. Fish and Wildlife Service (FWS) and USGS to learn more about how nutrient loading is influencing the biological carbon resource of the mangroves at J.N. "Ding" Darling National Wildlife Refuge (NWR), and whether local-scale management might provide intervention to offset any projected changes. We thank Scott Covington (FWS), Paul Tritaik (FWS), Kevin Godsea (FWS), Erin Myers (FWS), Mark Danaher (FWS), Kurt Johnson (FWS), Avery Renshaw (FWS), Dr. Emily Pindilli (USGS), Dr. Ilka Candy Feller (Smithsonian Institute), Dr. Darren J. Johnson (USGS), Dr. Jennifer Cartwright (USGS), and Nicole Cormier (Macquarie University) for project support, land management insight, field assistance, and/or feedback on study design. Dr. Danielle Ogurcak (Florida International University) and Mark Danaher provided reviews of a previous report draft. Funding was provided by the USGS LandCarbon Program and USGS Southeast Climate Adaptation Science Center, with supplementary funding from USGS Land Management Research Program and USGS Climate R&D Program. Any use of trade, firm, or product names is for descriptive purposes only and does not imply endorsement by the U.S. Government.

References Cited

Alongi, D.M., 2009, The Energetics of Mangrove Forests: New York, Springer.

Baldocchi, D., 2003, Assessing the eddy covariance technique for evaluating carbon dioxide exchange rates of ecosystems: past, present and future: Global Change Biology, v. 9, p. 479–492.

Beaulieu, J.J., DelSontro, T., and Downing, J.A., 2019, Eutrophication will increase methane emissions from lakes and impoundments during the 21st century: Nature Communications, v. 10, 1375.

Bovard, B.D., Curtis, P.S., Vogel, C.S., Su, H.-B., and Schmid, H.P., 2005, Environmental controls on sap flow in a northern hardwood forest: Tree Physiology, v. 25, p. 31–38.

Breithaupt, J.L., Smoak, J.M., Byrne, R.H., Waters, M.N., Moyer, R.P., and Sanders, C.J., 2018, Avoiding timescale bias in assessments of coastal wetland vertical change: Limnology and Oceanography, v. 63, p. S477–S495.

Bricker, S.B., Clement, C.G., Pirhalla, D.E., Orlando, S.P., and Forrow, D.R.G., 1999, National estuarine eutrophication assessment: effects of nutrient enrichment in the Nation's estuaries: Silver Springs, National Oceanic and Atmospheric Administration, Special Projects Office, 71 p.

Buffington, K.J., MacKenzie, R.A., Carr, J.A., Apwong, M., Krauss, K.A., and Thorne, K.M., 2021, Mangrove species' response to sea-lever rise across Pohnpei, Federated States of Micronesia: Reston, Open-File Report 2021-1002.

Bunting, P., Rosenqvist, A., Lucas, R.M., Rebelo, L.-M., Hilarides, L., Thomas, N., Hardy, A., Itoh, T., Shimada, M., and Finlayson, C.M., 2018, The Global Mangrove Watch – A new 2010 global baseline of mangrove extent: Remote Sensing, v. 10, 1669.

Buzzelli, C., Doering, P., Wan, Y., and Sun, D., 2014, Modeling ecosystem processes with variable freshwater inflow to the Caloosahatchee River Estuary, southwest Florida. II. Nutrient loading, submarine light, and seagrasses: Estuarine Coastal and Shelf Science, v. 151, p. 272–284.

Cahoon, D.R., and Lynch, J.C., 1997, Vertical accretion and shallow subsidence in a mangrove forest of southwestern Florida, U.S.A.: Mangroves and Salt Marshes, v. 1, p. 173–186.

Cahoon, D.R., and Reed, D.J., 1995, Relationships among marsh surface topography, hydroperiod, and soil accretion in a deteriorating Louisiana salt marsh: Journal of Coastal Research, v. 11, p. 357–369.

Cahoon, D.R., Lynch, J.C., Perez, B., Segura, B., Holland, R., Stelly, C., Stephenson, G., and Hensel, P., 2002, High-precision measurements of wetland sediment elevation: II. The rod surface elevation table: Journal of Sedimentary Research, v. 72, p. 734–739.

Callaway, J.C., Cahoon, D.R., and Lynch, J.C., 2013, The surface elevation table-marker horizon method for measuring wetland accretion and elevation dynamics, *in* DeLaune, R.D., Reddy, K.R., Richardson, C.J., and Megonigal, J.P., eds., Methods in Biogeochemistry of Wetlands: Madison, Soil Science Society of America, p. 901–917.

Carvajal, M., Cooke, D.T., and Clarkson, D.T., 1996, Responses of wheat plants to nutrient deprivation may involve the regulation of water-channel function: Planta, v. 199, p. 372–381.

Castaneda-Moya, E., Twilley, R.R., Rivera-Monroy, V.H., Marx, B.D., Coronado-Molina, C., and Ewe, S.M.L., 2011, Patterns of root dynamics in mangrove forests along environmental gradients in the Florida Coastal Everglades, USA: Ecosystems, v. 14, p. 1178–1195.

Čermák, J., Kučera, J., and Nadezhdina, N., 2004, Sap flow measurements with some thermodynamic methods, flow integration within trees and scaling up from sample trees to entire stands: Trees Structure and Function, v. 18, p. 529–546.

Chen, R., and Twilley, R.R., 1999, A simulation model of organic matter and nutrient accumulation in mangrove wetland soils: Biogeochemistry, v. 44, p. 93–118.

Clarkson, D.T., Carvajal, M., Henzler, T., Waterhouse, R.N., Smyth, A.J., Cooker, D.T., and Steudle, E., 2000, Root hydraulic conductance: diurnal aquaporin expression and the effects of nutrient stress: Journal of Experimental Botany, v. 51, p. 61–70.

Conrad, J.R., 2022, The effects of nutrient inputs on surface elevation change processes in tidal mangrove forests: Boca Raton, Florida Atlantic University, Ph.D. dissertation.

Cormier, N., Krauss, K.W., Demopoulos, A.W.J., Jessen, B.J., McClain-Counts, J.P., From, A.S., Flynn, L.L., 2022, Potential for carbon and nitrogen sequestration by restoring tidal connectivity and enhancing soil surface elevations in denuded and degraded south Florida mangrove ecosystems, *in* Krauss, K.W., Zhu, Z., and Stagg, C.L., eds., Wetland Carbon and Environmental Management: New Jersey, Wiley, p. 143–158.

DeGrove, B., 1981, Caloosahatchee River waste load allocation documentation: Water Quality Technical Series 2, Number 52, Florida Department of Environmental Regulation. 17 p.

Douglas, M.S., 1997, The Everglades: River of Grass, 50th Anniversary Edition: Sarasota, Pineapple Press, Inc., 478. p.

Drexler, J.Z., Krauss, K.W., Sasser, M.C., Fuller, C.C., Swarzenski, C.M., Powell, A., Swanson, K.M., and Orlando, J., 2013, A long-term comparison of carbon sequestration rates in impounded and naturally tidal freshwater marshes along the lower Waccamaw River, South Carolina: Wetlands, v. 33, p. 965–974.

Drexler, J.Z., Fuller, C.C., Orlando, J., and Moore, P., 2015, Recent rates of carbon accumulation in montane fens of Yosemite National Park, California, USA: Arctic, Antarctic, and Alpine Research, v. 47, p. 657–669.

Faron, N.T., 2021, The impact of nutrient loading on the soil and root respiration rates of Florida mangroves: Boca Raton, Florida Atlantic University, M.S. thesis.

Feller, I.C., 1995, Effects of nutrient enrichment on growth and herbivory of dwarf red mangrove (*Rhizophora mangle*): Ecological Monographs, v. 65, p. 477–505.

Feller, I.C., McKee, K.L., Wingham, D.F., and O'Neill, J.P., 2002, Nitrogen vs. phosphorus limitation across an ecotonal gradient in a mangrove forest: Biogeochemistry, v. 62, p. 145–175.

Feller, I.C., Wigham, D.F., McKee, K.L., Lovelock, C.E., 2003, Nitrogen limitation of growth and nutrient dynamics in a disturbed mangrove forest, Indian River Lagoon, Florida: Oecologia, v. 134, p. 405–414.

Florida Fish and Wildlife Conservation Commissions (FWC), 2005, Florida's Mangroves: Fish and Wildlife Research Institute Pamphlet, Tallahassee, Florida, USA.

Giri, C., Ochieng, E., Tieszen, L.L., Zhu, Z., Singh, A., Loveland, T., Masek, J., and Duke, N.C., 2011, Status and distribution of mangrove forests of the world using earth observation satellite data: Global Ecology and Biogeography, v. 20, p. 154–159.

Granier, A., 1987, Evaluation of transpiration in a Douglas-fir stand by means of sap flow measurements: Tree Physiology, v. 3, p. 309–320.

Hien, H.T., Marchand, C., Aime, J., and Cuc, N.T.K., 2018, Seasonal variability of CO_2 emissions from sediments in planted mangroves (Northern Vietnam): Estuarine, Coastal and Shelf Science, v. 213, p. 28–39.

Holm, G.O., Jr., Perez, B.P., McWhorter, D.E., Krauss, K.W., Johnson, D.J., Raynie, R.C., and Killebrew, C.J., 2016, Ecosystem level methane fluxes from tidal freshwater and brackish marshes of the Mississippi River Delta: implications for coastal wetland carbon projects: Wetlands, v. 36, p. 401–413.

Krauss, K.W., 2004, Growth, photosynthetic, and water use characteristics of south Florida mangrove vegetation in response to varying hydroperiod: Lafayette, University of Louisiana at Lafayette, Ph.D. dissertation.

Krauss, K.W., and Osland, M.J., 2022, Tropical cyclones and the organization of mangrove forests: a review: Annals of Botany, v. 125, p. 213–234.

Krauss, K.W., Doyle, T.W., Twilley, R.R., Rivera-Monroy, V.H., and Sullivan, J.K., 2006, Evaluating the relative contributions of hydroperiod and soil fertility on growth of south Florida mangroves: Hydrobiologia, v. 569, p. 311–324.

Krauss, K.W., Young, P.J., Chambers, J.L., Doyle, T.W., and Twilley, R.R., 2007, Sap flow characteristics of neotropical mangroves in flooded and drained soils: Tree Physiology, v. 27, p. 775–783.

Krauss, K.W., McKee, K.L., Lovelock, C.E., Cahoon, D.R., Saintilan, N., Reef, R., and Chen L., 2014, How mangrove forests adjust to rising sea level: New Phytologist, v. 202, p. 19–34.

Krauss, K.W., Barr, J.G., Engel, V., Fuentes, J.D., and Wang, H., 2015a, Approximations of stand water use versus evapotranspiration from three mangrove forests in southwest Florida, USA: Agricultural and Forest Meteorology, v. 213, p. 291–303.

Krauss, K.W., Duberstein, J.A., and Conner, W.H., 2015b, Assessing stand water use in four coastal wetland forests using sapflow techniques: annual estimates, errors and associated uncertainties: Hydrological Processes, v. 29, p. 112–127.

Krauss, K.W., Demopoulos, A.W.J., Cormier, N., From, A.S., McClain-Counts, J.P., and Lewis, R.R., III, 2018a, Ghost forests of Marco Island: Mangrove mortality driven by belowground soil structural shifts during tidal hydrologic alteration: Estuarine Coastal and Shelf Science, v. 212, p. 51–62.

Krauss, K.W., Noe, G.B., Duberstein, J.A., Conner, W.H., Stagg, C.L., Cormier, N., Jones, M.C., Bernhardt, C.E., Lockaby, B.G., From, A.S., Doyle, T.W., Day, R.H., Ensign, S.H., Pierfelice, K.N., Hupp, C.R., Chow, A.T., and Whitbeck, J.L., 2018b, The role of the upper estuary in wetland blue carbon storage and flux: Global Biogeochemical Cycles, v. 32, p. 817–839.

Krauss, K.W., Lovelock, C.E., Chen, L., Berger, U., Ball, M.C., Reef, R., Peters, R., Bowen, H., Vovides, A.G., Ward, E.J., Wimmler, M.-C., Carr, J., Bunting, P., and Duberstein, J.A., 2022a, Mangroves provide blue carbon ecological value at a low freshwater cost: Scientific Reports, v. 12, 17636.

Krauss, K.W., Zhu, Z., and Stagg, C.L., 2022b, Wetland Carbon and Environmental Management: Hoboken, New Jersey, Wiley and Sons, Inc and American Geophysical Union.

Krauss, K.W., Whelan, K.R.T., Kennedy, J.P., Friess, D.A., Rogers, C.S., Stewart, H.A., Grimes, K.W., Trench, C.A., Ogurcak, D.E., Toline, C.A., Ball, L.C., and From, A.S., 2023, Framework for facilitating mangrove recovery after hurricanes on Caribbean islands: Restoration Ecology (in press).

Lahmann, E.J., 1988, Effects of different hydrological regimes on the productivity of *Rhizophora mangle* L.: a case study of mosquito control impoundments at Hutchinson Island, Saint Lucie County, Florida: Coral Gables, University of Miami, Ph.D. dissertation.

LaPointe, B.E., and Bedford, B.J., 2007, Drift rhodophyte blooms emerge in Lee County, Florida, USA: evidence of escalating coastal eutrophication: Harmful Algae, v. 6, p. 421–437.

Lee County, 2019, Caloosahatchee – North Fort Meyers Nutrient and Bacteria Source Identification Study. Lee County Board of County Commissioners Workshop.

Lewis, R.R., Milbrandt, E.C., Brown, B., Krauss, K.W., Rovai, A.S., Beever J.W. III, and Flynn, L.L., 2016, Stress in mangrove forests: early detection and preemptive rehabilitation are essential for future successful worldwide mangrove forest management: Marine Pollution Bulletin, v. 109, p. 764–771.

Liang, J., Farquhar, G.D., and Ball, M.C., 2022, Water use efficiency in mangroves: conservation of water use efficiency determined by stomatal behavior across leaves, plants, and forests: Advances in Botanical Research, v. 103, p. 43–59.

Linderson, M.-L., Mikkelsen, T.N., Ibrom, A., Lindroth, A., Ro-Poulsen, H., and Pilegaard, 2012, Up-scaling of water use efficiency from leaf to canopy as based on leaf gas exchange relationships and the modeled in-canopy light distribution: Agricultural and Forest Meteorology, v. 152, p. 201–211.

Liu, Z., Choudhury, S.H., Xia, M., Holt, J., Wallen, C.M., Yuk, S., and Sanborn, S.C., 2009, Water quality assessment of coastal Caloosahatchee River watershed, Florida: Journal of Environmental Science and Health (Part A), v. 44, p. 972–984.

Lovelock, C.E., 2008, Soil respiration and belowground carbon allocation in mangrove forests: Ecosystems, v. 11, p. 342–354.

Lovelock, C.E., Adame, M.F., Bennion, V., Hayes, M., O'Mara, J., Reef, R., and Santini, N.S., 2014a, Contemporary rates of carbon sequestration through vertical accretion of sediments in mangrove forests and saltmarshes of South East Queensland, Australia: Estuaries and Coasts, v. 37, p. 763–771.

Lovelock, C.E., Feller, I.C., Reef, R., Ruess, R.W., 2014b, Variable effects of nutrient enrichment on soil respiration in mangrove forests: Plant and Soil, v. 79, p. 135–148.

Lugo, A.E., and Snedaker, S.C., 1974, Ecology of mangroves: Annual Review of Ecology and Systematics, v. 5, p. 39–64.

Lynch, A.J., Thompson, L.M., Morton, J.M., Beever, E.A., Clifford, M., Limpinsel, D., Magill, R.T., Magness, D.R., Melvin, T.A., Newman, R.A., Porath, M.T., Rahel, F.J., Reynolds, J.H., Schuurman, G.W., Sethi, S.A., Wilkening, 2022, RAD adaptive management for transforming ecosystems: BioScience, v. 72, p. 45–56.

Maher, D.T., Call, M., Santos, I.R., and Sanders, C.J., 2018, Beyond burial: lateral exchange is a significant atmospheric carbon sink in mangrove forests: Biology Letters, v. 14, 20180200.

McKee, K.L., 2011, Biophysical controls on accretion and elevation change in Caribbean mangrove ecosystems: Estuarine, Coastal and Shelf Science, v. 91, p. 475–483.

McKee, K.L., Cahoon, D.R., and Feller, I.C., 2007, Caribbean mangroves adjust to rising sea level through biotic controls on change in soil elevation: Global Ecology and Biogeography, v. 16, p. 545–556.

McKee, K.L., Feller, I.C., Popp, M., and Wanek, W., 2002, Mangrove isotopic fractionation ($d^{15}N$ and $d^{13}C$) across a nitrogen versus phosphorus limitation gradient: Ecology, v. 83, p. 1065–1075.

McKee, K.L., Krauss, K.W., Cahoon, D.R. 2020. Does geomorphology determine vulnerability of coasts to sea-level rise?, *in* Sidik, F., Friess, D.A., eds., Dynamic Sedimentary Environments of Mangrove Coasts: Amsterdam, Elsevier, p. 255-272.

McLaughlin, D.L., Brown, M.T., and Cohen, M.J., 2012, The ecohydrology or a pioneer wetland species and a drastically altered landscape: Ecohydrology, v. 5, p. 656–667.

Mcleod, E., Chmura, G.L., Bouillon, S., Salm, R., Björk, M., Duarte, C.M., Lovelock, C.E., Schlesinger, W.H., and Silliman, B.R., 2011, A blueprint for blue carbon: toward an improved understanding of the role of vegetated coastal habitats in sequestering CO_2: Frontiers in Ecology and the Environment, v. 9, p. 552–560.

Meyers, J.M., Langtimm, C.A., Smith, T.J., III, and Pednault-Willett, K., 2006, Wildlife and Habitat Damage Assessment from Hurricane Charley: Recommendations for Recovery of the J.N. "Ding" Darling National Wildlife Refuge Complex: U.S. Geological Survey, Open File Report 2006-1126, Reston, Virginia, USA. 91 p.

Milbrandt, E.C., Greenawalt-Boswell, J.M., Sokoloff, P.D., and Bartone, S.A., 2006, Impact and response of southwest Florida mangroves to the 2004 hurricane season: Estuaries and Coasts, v. 29, p. 979–984.

Miller, H., 2022, Water use and nutrient retention in fertilized black and red mangroves in southwest Florida: Clemson, Clemson University, M.S. thesis.

Noe, G.B., Hupp, C.R., Bernhardt, C.E., and Krauss, K.W., 2016, Contemporary deposition and long-term accumulation of sediment and nutrients by tidal freshwater forested wetlands impacted by sea level rise: Estuaries and Coasts, v. 39, p. 1006–1019.

Osland, M.J., Spivak, A.C., Nestlerode, J.A., Lessmann, J.M., Almario, A.E., Heitmuller, P.T., Russell, M.J., Krauss, K.W., Alverez, F., Dantin, D.D., Harvey, J.E., From, A.S., Cormier, N., and Stagg, C.L., 2012, Ecosystem development after mangrove creation: plant-soil change across a 20-year chronosequence: Ecosystems, v. 15, p. 848–866.

Parkinson, R.W., and Wdowinski, S., 2022, Accelerating sea-level rise and the fate of mangrove plant communities in South Florida, U.S.A.: Geomorphology, v. 412, 108329.

Patterson, S.G., 1986, Mangrove Community Boundary Interpretation and Detection of Areal Changes on Marco Island, Florida: Application of Digital Image Processing and Remote Sensing Techniques: Washington, D.C., Biological Report 86(10), U.S. Fish and Wildlife Service.

Peneva-Reed, E.I., and Zhiliang, Z., 2019, Mangrove Data Collected from J.N. "Ding" Darling National Wildlife Refuge, Sanibel Island, Florida, United States: U.S. Geological Survey data release, https://doi.org/10.5066/P9P2PHU3.

Peneva-Reed, E.I., Krauss, K.W., Bullock, E.L., Zhu, Z., Woltz, V.L., Drexler, J.Z., Conrad, J.R., and Stehman, S.V., 2021, Carbon stock losses and recovery observed for a mangrove ecosystem following a major hurricane in Southwest Florida: Estuarine, Coastal and Shelf Science, v. 248, 106750.

Poffenbarger, H.J., Needelman, B.A., and Megonigal, J.P., 2011, Salinity influence on methane emissions from tidal marshes: Wetlands, v. 31, p. 831–842.

Reef, R., Feller, I.C., and Lovelock, C.E., 2010, Nutrition of mangroves: Tree Physiology, v. 30, p. 1148–1160.

Robert, E.M.R., Koedam, N., Beeckman, H., and Schmitz, N., 2009, A safe hydraulic architecture as wood anatomical explanation for the differences in distribution of the mangroves Avicennia and Rhizophora: Functional Ecology, v. 23, p. 649–657.

Rogers, K., Kelleway, J.J., Saintilan, N., Megonigal, J.P., Adams, J.B., Holmquist, J.R., Lu, M., Schile-Beers, L., Zawadzki, A., Mazumder, D., and Woodroffe, C.D., 2019, Wetland carbon storage controlled by millennial-scale variation in relative sea-level rise: Nature, v. 567, p. 91–95.

Shoemaker, W.B., Anderson, F.E., Sirianni, M.J., and Daniels, A., 2022, Carbon fluxes and potential soil accumulation within Greater Everglades cypress and pine forested wetlands, *in* Krauss, K.W., Zhu, Z., and Stagg, C.L., eds., Wetland Carbon and Environmental Management: New Jersey, Wiley, p. 371–384.

Smoak, J.M., Breithaupt, J.L., Smith, T.J., III, and Sanders, C.J., 2013, Sediment accretion and organic carbon burial relative to sea-level rise and storm events in two mangrove forests in Everglades National Park: Catena, v. 104, p. 58–66.

Troxler, T.G., Barr, J.G., Fuentes, J.D., Engel, V., Anderson, G., Sanchez, C., Lagomasino, D., Price, R., and Davis, S.E., 2015, Component-specific dynamics of riverine mangrove CO_2 efflux in the Florida coastal Everglades: Agricultural and Forest Meteorology, v. 213, p. 273–282.

Zhao, H., Yang, S., Guo, X., Peng, C., Gu, X., Deng, C., and Chen, L., 2018, Anatomical explanations for acute depressions in radial patterns of axial sap flow in two diffuse-porous mangrove species: implications for water use: Tree Physiology, v., 38, p. 276–286.

Appendix 1. Accounting of Study Methods Used

This report presents an overview of studies to understand the role that current and future additional loading of nitrogen and phosphorus may have on a valuable mangrove resource at Ding Darling National Wildlife Refuge. Much of the data collection reported herein was from one Ph.D. dissertation (Conrad, 2022) and two M.S. theses (Faron, 2021; Miller, 2022), augmented by a number of smaller studies. These graduate products provide greater information on specific procedures used in this report as well as results from additional data collection. We summarize the salient points in this report. Along with these three resources, additional procedural references are provided in **Table 1-1**.

Table 1-1. References used to develop techniques used in this report, with citations provided tabularly in lieu of the References Cited section of the Appendices (p. 41).

Technique[1]	Reference	Citation
SET-MH	Cahoon, Lynch, and others (2002)	*J. Sedimentary Res.*, v. 72, p. 734–739
SET-MH	McKee, Cahoon, Feller (2007)	*Glob. Ecol. Biogeogr.*, v. 16, p. 545–556
SET-MH	Callaway, Cahoon, Lynch (2013)	*Methods in Biogeochem. Wetlands*, p. 901–917
SET-MH	Cahoon (2015)	*Estuaries Coasts*, v. 38, p. 1077–1084
Coring	Lynch, Meriwether, and others (1989)	*Estuaries*, v. 12, p. 284–299
Coring	Drexler, Fuller, and others (2015)	*Arctic Antarctic Alpine Res.*, v. 47, p. 657–669
Coring	Drexler, Fuller, Archfield (2018)	*Quaternary Sci. Rev.,* v. 199, p. 83–96
Soil CO_2 flux	Lovelock (2008)	*Ecosystems,* v. 11, p. 342–354
Soil CO_2 flux	Krauss and Whitbeck (2012)	*Wetlands,* v. 32, p. 73–81
Soil CO_2 flux	Jin, Lu, Ye, Ye (2013)	*Pedosphere*, v. 23, p. 678–685
Soil CO_2 flux	Batson, Noe, and others (2015)	*J. Geophys. Res. Biogeosci.,* v. 120, p. 77–95
Pneu CO_2 flux	Kramer, Riley, Bannister (1952)	*Ecology*, v. 33, p. 117–121
Pneu CO_2 flux	Scholander (1955)	*American J. Bot.,* v. 42, p. 92–98
Pneu CO_2 flux	Troxler, Barr, and others (2015)	*Agri. For. Meteorol.,* v. 213, p. 273–282
TDP Sapflow	Granier (1987)	*Tree Physiol.*, v. 3, p. 309–320
TDP Sapflow	Zimmermann, Zhu, and others (1994)	*Botanica Acta,* v. 107, p. 218–229
TDP Sapflow	Krauss, Young, and others (2007)	*Tree Physiol.*, v. 27, p. 775–783
TDP Sapflow	Krauss, McKee, Hester (2014)	*Ecohydrol.*, v. 7, p. 354–365
Stand *S*	Wullschleger, Hanson, Todd (2001)	*For. Ecol. Manage.,* 143, p. 205–213
Stand *S*	Oishi, Oren, Stoy (2008)	*Agri. For. Meteorol.,* v. 148, p. 1719–1732
Stand *S*	Krauss, Duberstein, Conner (2015)	*Hydrol. Processes,* v. 29, p. 112–127
Stand *S*	Krauss, Barr, and others (2015)	*Agri. For. Meteorol.,* v. 213, p. 291–303
Stand *S*	Allen, Krauss, and others (2016)	*J. Geophys. Res. Biogeosci.,* v. 121, p. 753–766
Stand *S*	Wullschleger, Hanson, Todd (2001)	*For. Ecol. Manage.,* v. 143, p. 205–213
NEE_c	Beer, Reichstein, and others (2007)	*Geophy. Res. Letts., v.* 34, L05401
NEE_c	Linderson, Mikkelsen, and others (2008)	*Geophys. Res. Abstracts.,* v. 10, EGU2008-A-09322
NEE_c	Barr, Engel, and others (2010)	*J. Geophys. Res. Biogeosci.,* v. 115, G02020
NEE_c	Linderson, Mikkelsen, and others (2012)	*Agri. For. Meteorol.,* v. 152, p. 201–211
NEE_c	Krauss, Lovelock, and others (2022)	*Scientific Reports,* v. 12, 17636
SLR Modeling	Buffington, MacKenzie and others (2021)	*USGS Open-File Report 2021–1002*
SLR Modeling	Swanson, Drexler, and others (2014)	*Estuaries and Coasts*, v. 37, p. 476–492

[1]SET-MH = Surface Elevation Table – Marker Horizon Technique; TDP = Thermal Dissipation Probe; Stand *S* = Stand water use, assumed to equate to canopy transpiration; NEE_c = Net Ecosystem Exchange of Carbon; SLR = Sea-level rise

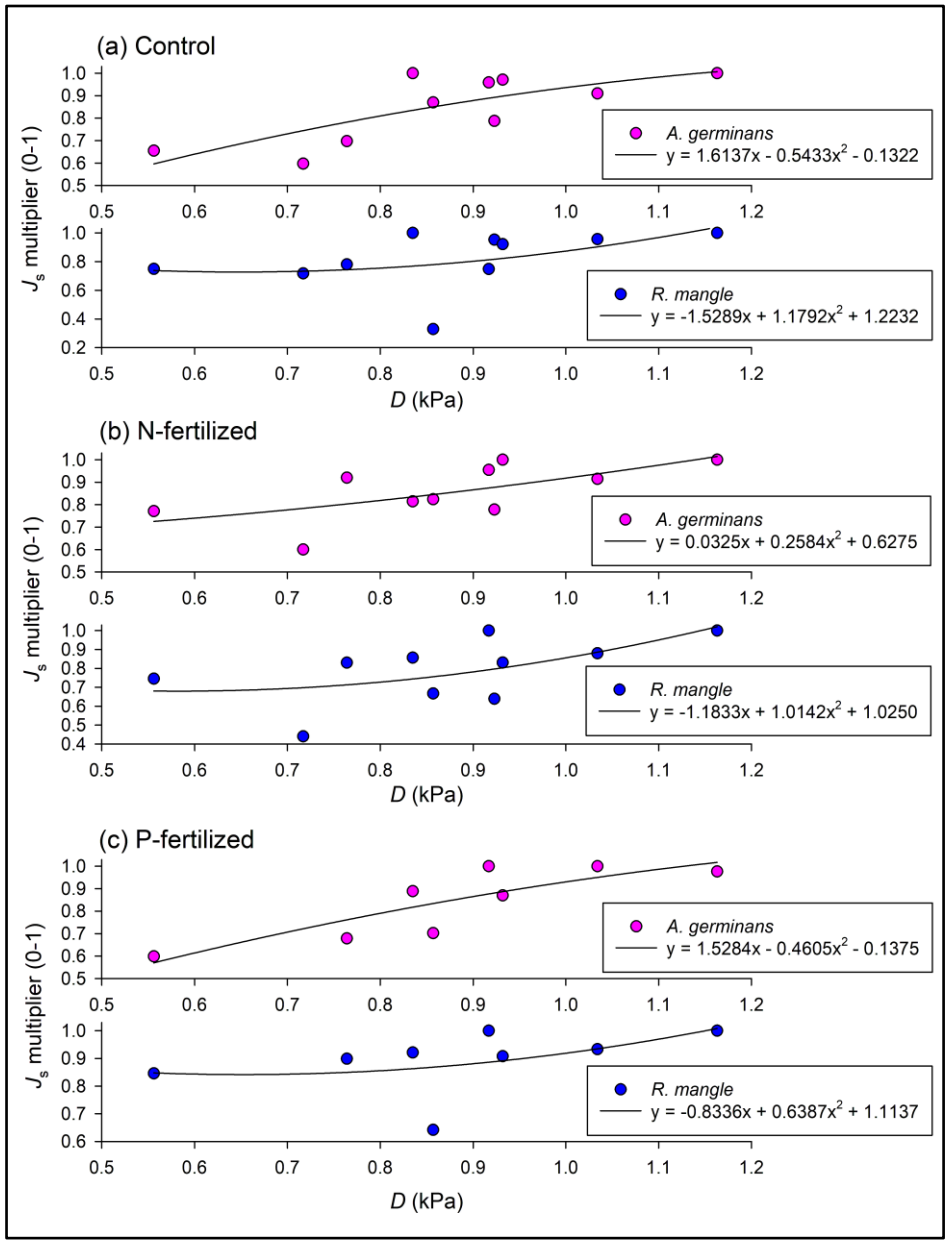

Figure 1-1. Polynomial relationships between average vapor pressure deficit (*D*, kPa) from DDNWR weather station and sap flow (J_s) multiplier (0-1) to verify model application for Control (**a**), N-fertilized (**b**), and P-fertilized (**c**) trees of *Avicennia germinans* (pink dots) and *Rhizophora mangle* (blue dots).

As an important point of verification of water transport theory, exploring relationships between vapor pressure deficit (*D*) and sap flow (J_s) is an inherent first step in sap flow analysis. We investigate this relationship by reducing the range of J_s values to a multiplier for better incorporation into our spreadsheet model (Krauss and others, 2015), and separate *D*-to-J_s by species (*Avicennia germinans*, *Rhizophora mangle*) and treatment (control, +N-fertilized, +P-fertilized) (**fig. 1-1**). A mangrove species and zone (basin, fringe) breakdown of how stand water use (*S*) varied by fertilization is also provided (**Table 1-2**).

Table 1-2. Zone × species breakdown of average *S* (mm H_2O/year) for each treatment. +N and +P treatment influences were not available for *L. racemosa* because no fertilized trees were measured.

Treatment	Zone	Species	*S*, average (mm H_2O/ year)
Control	Basin	*A. germinans*	321.6
Control	Basin	*L. racemosa*	190.7
Control	Basin	*R. mangle*	170.9
Control	Fringe	*A. germinans*	126.2
Control	Fringe	*L. racemosa*	164.2
Control	Fringe	*R. mangle*	330.5
+N	Basin	*A. germinans*	301.0
+N	Basin	*R. mangle*	160.1
+N	Fringe	*A. germinans*	118.5
+N	Fringe	*R. mangle*	329.4
+P	Basin	*A. germinans*	287.1
+P	Basin	*R. mangle*	197.0
+P	Fringe	*A. germinans*	69.2
+P	Fringe	*R. mangle*	428.1

Appendix 2. Modeling Mangrove Response to Sea-level Rise

Mangrove species have different adaptation strategies to sea-level rise, which include variable aerial root morphologies and developmental growth patterns, belowground root-to-volume and lignin-to-nitrogen ratios, and sediment trapping and retention properties (Snedaker, 1995; McKee, 2011; Krauss and others, 2014; Chen and others, 2022), which influence model outcome. Sea-level rise models are obligated to include all known processes that contribute to wetland response. As such, a suite of models has been developed over the past two decades that transition from bathtub approaches that make use of static elevations that overpredict losses, to models that incorporate in-situ biologic and sedimentary feed-back responses to sea-level change (Kirwan and others, 2010; Kirwan and others, 2016). As sea levels rise, mangrove wetlands respond in different ways to build vertical elevations (Krauss and others 2014). One such model that incorporates feedbacks is the Wetland Accretion Rate Model of Ecosystem Resilience (WARMER)-Mangroves, which makes use of a soil cohort approach that balances soil inputs and losses to decomposition as hydrology changes over time, while tracking changes in species composition (Buffington and others, 2021).

Starting elevation for intertidal and supratidal soils on Sanibel Island was derived at a spatial resolution of 5 m by expanding Lidar Elevation Adjustment with NDVI, or a LEAN-corrected, DEM (digital elevation model) coverage to Sanibel Island (Buffington and Thorne, 2023). Soil bulk density, organic matter, and radioisotope dating of Sanibel Island's basin mangroves were incorporated into WARMER-Mangroves (Drexler, 2019), as were data for contemporary surface elevation change (from surface-elevation tables), forest structure across the refuge, litterfall productivity, tree diameter growth rates, root productivity, and hydroperiod (Peneva-Reed and Zhu, 2019; Peneva-Reed and others, 2021; Conrad, 2022). Root size class characterization was initialized with data from the Everglades (Castañeda-Moya and others, 2011) and updated with data from Sanibel Island where possible (Conrad, 2022).

WARMER-Mangroves simulated soil development as mangroves respond to changing hydroperiod from sea-level rise (Buffington and others, 2021). We chose to include only *Avicenna* and *Rhizophora* mangroves (**fig. 2-1**), as they were by far the most common species across Sanibel Island (Peneva-Reed and Zhu, 2019), and even when *Laguncularia racemosa* was present, *Avicennia* and *Rhizophora* generally dominated. Since fringe mangroves are more exposed to processes not considered in the model, such as wind-wave dynamics, we opted to focus our attention on basin mangroves; radioisotope dating of soil cores was also unsuccessful in fringe habitats due to extremely high carbonate content of fringe sediments and extensive mixing in the depth profile, eliminating a crucial calibration dataset. We choose to model as a single basin mangrove habitat, as *Avicenna* and *Rhizophora* mangroves were well mixed across Sanibel Island (Peneva-Reed and Zhu 2019), and we lacked several species-specific model parameters. Hydroperiod data were obtained from nearby monitoring stations. We assumed that relative flooding frequency from basin and fringe water level loggers represented the niche of *A. germinans* and *R. mangle*,

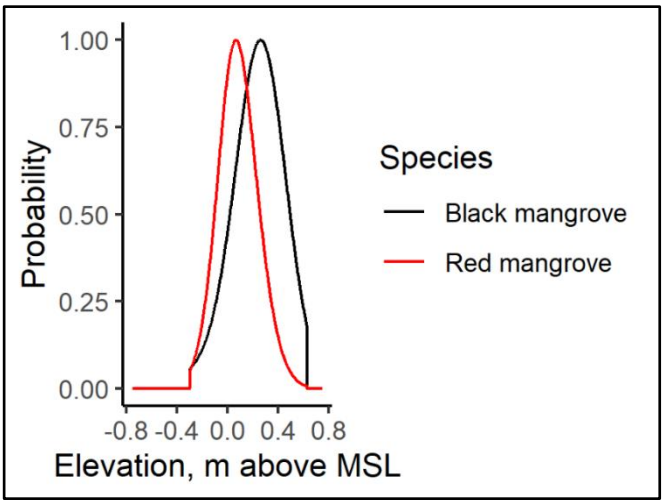

Figure 2-1. Approximate extent of mangroves across DDNWR and initial mangrove species dominance (black, *Avicennia germinans*; red, *Rhizophora mangle*) as calculated by the model (WARMER-Mangroves).

respectively, based on elevation differences (**fig. 2-2**); this assumption resulted in reasonable distributions of both species at the start of sea-level rise projections.

Forest structure data were used to define carrying capacity in terms of basal area and to relate basal area to aboveground biomass (Peneva-Reed and Zhu, 2019). Tree diameter growth rates, derived from dendrometer measurements (Conrad, 2022) were modified by a niche coefficient, here assumed to be a unimodal curve stretched across the elevation range where mangroves were observed (-28 to 45 cm, MSL). Total belowground biomass was calculated with established root-to-shoot ratios (Peneva-Reed and Zhu, 2019) and then split into three size classes with unique turnover rates. Dead organic matter was divided into labile and refractory pools, with refractory decomposition set at a constant 0.005%. The rate of labile decomposition was set at a constant decay coefficient of 0.002 d^{-1} (Simpson and others, 2023). The rate of mineral-associated organic matter production was determined through model calibration and by comparing modeled and observed organic accumulation rates from dated soil cores (Drexler, 2019). Soil cores were also used to calibrate the mineral sediment deposition rate, which was a function of hydroperiod. The 2 cm sections from the soil cores defined the relationship between soil organic matter and bulk density. Further model details and formulations can be found in Buffington and others (2021).

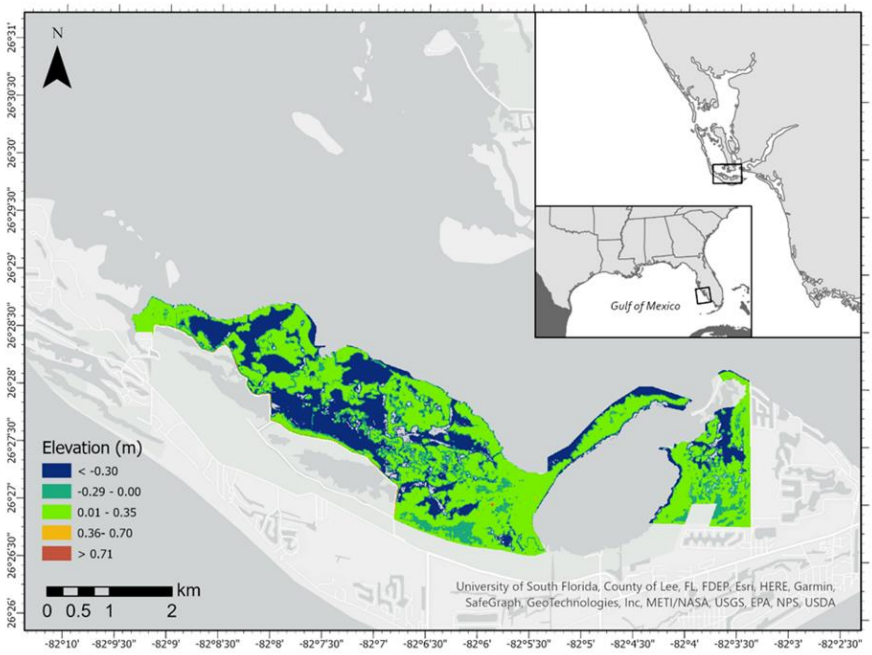

Figure 2-2. Bias-corrected elevation (m, NAVD88) of mangrove swamp study domain across the Ding Darling NWR. The study domain was selected based on intact mangrove forest and natural hydrology.

As parameterized, using data from local or nearby mangrove forests, WARMER-Mangroves was unable to achieve the 50-year accretion rates estimated from soil cores. Thus, an additional feedback mechanism was implemented to increase organic accumulation rates. Shoot:root ratios from the literature were assumed to be at the elevation of optimum suitability. Shoot:root ratios decreased as flooding went up, while shoot:root ratios increased as flooding went down. The slope of a linear adjustment to shoot:root versus elevation, describing the speed at which mangroves adjusted to their new elevation, became an additional tuning parameter that facilitated much better calibration to the soil core data. The primary assumption of this mechanism is that mangroves increase their root production with greater long-term inundation, perhaps to maintain a favorable position in the tidal frame. This assumption is supported by work in mangroves across the Caribbean (Castañeda-Moya and others, 2011; McKee and others, 2007; McKee, 2011) and globally (Rogers and others, 2019). Model parameters are summarized in **Table 2-1**.

Table 2-1. Parameters used for WARMER-Mangroves.

Parameter	Value	Units	Source
Suspended sediment concentration	5.9	mg/L	Calibration
Tide range	0.71	m	NOAA gauge
Structural root fraction	0.4	-	Conrad, 2022
Fine root fraction	0.192	-	Conrad, 2022
Maximum tree density	0.0036	m^2/m^2	Peneva-Reed and Zhu, 2019
Root growth depth	0.7	m	Estimated
Root:shoot	0.235	-	Peneva-Reed and Zhu, 2019
MAOM production rate	0.05	y^{-1}	Calibration
Fine root turnover	0.63	y^{-1}	Conrad, 2022
Large root turnover	0.13	y^{-1}	Conrad, 2022
Structural root turnover	0.05	y^{-1}	Castañeda-Moya and others, 2011
Dead root particulate rate	0.15	y^{-1}	Calibration
Fine root labile fraction	0.36	-	McKee and others, 2007
Large root labile fraction	0.71	-	McKee and others, 2007
Leaf litter fraction	0.7	-	Aké-Castillo and others, 2006
Leaf refractory fraction	0.27	-	Middleton and McKee, 2001
Litter deposition fraction	0.05	-	Conrad, 2022; calibrated
Relative growth rate	0.136	y^{-1}	Conrad, 2022; calibrated
Labile decomposition	0.002	d^{-1}	Simpson and others, 2023
Refractory decomposition	0.005	% y^{-1}	Constant, this study
Wood litter burial rate	0.1	y^{-1}	Constant, this study
Dead fall rate	0.4	y^{-1}	Constant, this study

Appendix 3. Project Data Releases

Conrad, J.R., Krauss, K.W., Benscoter, B.P., and From, A.S., 2023, **Soil surface elevation change data from rod surface elevation tables (rSET) from mangrove forests at Ding Darling National Wildlife Refuge, Sanibel Island, Florida (2018-2022)**: U.S. Geological Survey data release, https://doi.org/10.5066/P9UJFBX8.

Abstract - This study monitored soil surface elevation change from mangrove forests fertilized with nitrogen and phosphorus from 2018-2021. The mangroves selected at Ding Darling National Wildlife Refuge (NWR) have been previously exposed to high nutrient loading from agricultural discharge into the Caloosahatchee River, which elevated soil phosphorus levels to 3-4 times ambient before treatments were imposed. Sea-level rise vulnerability with additional nitrogen and phosphorus is a concern for these mangrove ecosystems.

Benscoter, B.P., and Faron, N.T., 2023, **Soil and pneumatophore CO_2 flux data by nutrient treatment (N, P) for mangroves of Ding Darling NWR, Sanibel Island, Florida (2020)**: U.S. Geological Survey data release, https://doi.org/10.5066/P9BMLWRB.

Abstract - This study evaluated CO_2 flux from soils and pneumatophore fluxes from *Avicennia germinans* mangrove trees subjected to nitrogen and phosphorus fertilization versus an unfertilized control within a basin mangrove ecosystem. Data were collected twice, once in the summer (June 2020) and once in the winter (November 2020) and will be used to help develop a carbon budget for basin mangroves on Sanibel Island, Florida.

Duberstein, J.A., Ward, E.J., Krauss, K.W., Conrad, J.R., Miller, H., and From, A.S., 2023, **Sap flow, leaf water use efficiency, and partial weather station data to support stand water use modeling by nutrient treatment (N, P) for mangroves of Ding Darling NWR, Sanibel Island, Florida (2019-2020)**: U.S. Geological Survey data release, https://doi.org/10.5066/P9M9F5UM.

Abstract - This study evaluated sap flow of neotropical mangrove species subjected to background nutrient loading, and well as fertilization with either nitrogen or phosphorus, at Ding Darling National Wildlife Refuge (NWR). Data collections were made seasonally to model stand water use by mangrove forest type as a metric of ecosystem stress through alteration of water use potential at the stand level. Data on leaf-scale water use efficiency, and data from a partial weather station deployed near study sites, were included for enabling model development and calculation of stand water use.

Buffington, K.J., and Thorne, K.M., 2023, **Bias-corrected topobathymetric elevation model for south Florida, 2018**: USGS Data Release, https://doi.org/10.5066/P9KV6FMQ.

Abstract - Accurate elevation data in coastal ecosystems are crucial for understanding vulnerability to sea-level rise. LiDAR has become increasingly available; however, in tidal wetlands such as mangroves and salt marsh, vertical bias from dense vegetation reduces accuracy of the delivered 'base earth' products. To increase accuracy of elevation models across south Florida, we applied the LEAN technique to six different lidar collections from 2007-2018. On average, LEAN correction increased DEM accuracy by 46.1 percent, reducing the vertical bias. After correction and post-processing, the DEMs were merged together with a bathymetric dataset to create a seamless topo-bathy product.

Buffington, K.J., and Thorne, K.M., 2023, **Elevation and mangrove cover projections under sea-level rise scenarios at J.N. Ding Darling National Wildlife Refuge, Sanibel Island, Florida, 2020-2100**: USGS Data Release, https://doi.org/10.5066/P9GOTC10.

Abstract - Elevation projections from the WARMER-Mangroves model for J. N. "Ding" Darling National Wildlife Refuge across a range of sea-level rise scenarios (53, 115, and 183 cm by 2100) are reported. The model was calibrated using dated soil cores sampled from the basin hydrologic zone.

Buffington, K.J., and Thorne, K.M., 2022, **Elevation survey across southwest Florida coastal wetlands, 2021**: USGS Data Release: https://doi.org/10.5066/P9POUPH5.

Abstract - Accurate elevation data in coastal wetlands are crucial for planning for sea-level rise. Elevation surveys were conducted across southwest Florida wetlands to provide ground validation of LiDAR as well as target long-term monitoring stations (surface elevation tables). Surveys were conducted in June 2021 across Ding Darling National Wildlife Refuge, Clam Bay, Rookery Bay National Estuarine Research Reserve, and Ten Thousand Islands National Wildlife Refuge. A combination of post-processed kinematic GPS and differential levelling survey techniques were employed, depending on the canopy cover.

Peneva-Reed, E.I., and Zhu, Z., 2019, **Mangrove data collected from J.N. "Ding" Darling National Wildlife Refuge, Sanibel Island, Florida, United States**: USGS Data Release, https://doi.org/10.5066/P9P2PHU3.

Abstract - Mangrove inventory data from J.N. Ding Darling National Wildlife Refuge, Sanibel Island, Florida, USA collected in 2016 and 2017. Plot data include X and Y location, downed dead wood counts, mangrove species information, and site descriptions. Tree data include the three species found on the refuge: *Avicennia germinans* (black mangrove), *Laguncularia racemosa* (white mangrove) and *Rhizophora mangle* (red mangroves). Forest plots were inventoried for diameter at breast height (DBH), height, and mortality status.

Drexler, J., 2019, **Dry Weight, Volume and % Organic Carbon in Mangrove Sediment Cores Collected in September 2018 in J.N. "Ding" Darling National Wildlife Refuge, Sanibel Island, Florida, United States**: USGS Data Release, https://doi.org/10.5066/P9CFK79S.

Abstract - Sediment cores (1 m in depth) were collected at each of three mangrove sites at J.N. Ding Darling National Wildlife Refuge on Sanibel Island, Florida. At each site, one core was collected in the hydrogeomorphic zone called the fringe, which is the area directly adjacent to the ocean. The other core was collected in the zone called the basin, which is the large area, often behind a small berm, that receives less direct tidal energy. All cores were sectioned and measured for sectional volume, dry weight and % organic carbon (OC) by weight.

Appendix 4. Project Deliverables

Publications

Peneva-Reed, E.I., Krauss, K.W., Bullock, E.L., Zhu, Z., Woltz, V.L., Drexler, J.Z., Conrad, J.R., and Stehman, S.V., 2021, Carbon stock losses and recovery observed for a mangrove ecosystem following a major hurricane in Southwest Florida: Estuarine, Coastal and Shelf Science, v. 248, 106750, https://doi.org/10.1016/j.ecss.2020.106750

Faron, N.T., 2021, The Impact of Nutrient Loading on the Soil and Root Respiration Rates of Florida Mangroves: M.S. Thesis, Florida Atlantic University, 55 p.

Krauss, K.W., Zhu, Z, and Stagg, C.L., 2022, Wetland Carbon and Environmental Management: AGU Geophysical Monograph, Washington, DC, USA.

Miller, H., 2022, Water Use and Nutrient Retention in Black and Red Mangroves in Southwest Florida: M.S. Thesis, Clemson University, 80 p.

Krauss, K.W., Lovelock, C.E., Chen, L., Berger, U., Ball, M.C., Reef, R., Peters, R., Bowen, H., Vovides, A.G., Ward, E.J., Wimmler, M.-C., Carr, J., Bunting, P, and Duberstein, J.A., 2022, Mangroves provide blue carbon ecological value at a low freshwater cost: Scientific Reports, v. 12, 17636, https://doi.org/10.1038/s41598-022-21514-8

Temmerman, S., Horstman, E.M., Krauss, K.W., Mullarney J.C., Pelckmans, I., and Schoutens, K., 2023, Marshes and mangroves as nature-based coastal storm buffers: Annual Review of Marine Science, v. 15, p. 95–118, https://doi.org/10.1146/annurev-marine-040422-092951

Conrad, J.R., 2022, The effects of nutrient inputs on surface elevation change processes in tidal mangrove forests: Ph.D. Dissertation, Florida Atlantic University, 161 p.

Krauss, K.W., Whelan, K.R.T., Kennedy, J.P., Friess, D.A., Rogers, C.S., Stewart, H.H., Grimes, K.W., Trench, C.A., Ogurcak, D.E., Toline, C.A., Ball, L.C., and From, A.S., Framework for facilitating mangrove recovery after hurricanes on Caribbean islands: Restoration Ecology, v. 31, e13885, https://doi.org/10.1111/rec.13885

Feher, L.C., Osland, M.J., McKee, K.L., Whelan, K.R.T., Coronado-Molina, C., Sklar, F.H., Krauss, K.W., Howard, R.J., Cahoon, D.R., Lynch, J.C., Lamb-Wotton, L., Troxler, T.G., Conrad, J.R., Anderson, G.H., Vervaeke, W.C., and Smith, T.J. III., 2023, Soil elevation change in mangrove forests and marshes of the Greater Everglades: a regional synthesis of surface-elevation table-marker horizon (SET-MH) data. *Estuaries and Coasts* (in press), https://doi.org/10.1007/s12237-022-01141-2

Conrad, J.R., Krauss, K.W., Benscoter, B.W., Feller, I.C., Cormier, N., and Johnson, D.J., 2023, Eutrophication saturates surface elevation adjustment potential in tidal mangrove forests: Estuaries and Coasts (in review, **IP-153884**), Bureau Approval Date: 1 November 2023.

Presentations

Buffington, K., Thorne, K.M., Krauss, K.W., Savarese, M., and Sheng, Y.P., 2021, A new modeling approach (WARMER-Mangrove) to explore coastal wetland response to sea-level rise for southwest Florida, Greater Everglades Ecosystem Restoration Conference, 19-29 April, Virtual Conference.

Sheng, Y.P., et al., 2021, Assessing the role of NNBF for reducing coastal flood, wave, and property damage during storms in a changing climate, Greater Everglades Ecosystem Restoration Conference, 19-29 April, Virtual Conference.

Feher, L.C., et al., 2021, Coastal wetland soil elevation change in the Greater Everglades: A regional synthesis of surface elevation table-marker horizon (SET-MH) data, Greater Everglades Ecosystem Restoration Conference, 19-29 April, Virtual Conference.

MacKenzie, R.A., Krauss, K.W., Cormier, N., Eperiem, E., van Aardt, J., Karger, A.R., 2021, Monitoring mangrove response to sea level rise: ^{210}Pb, SETs, or LiDAR?, 26th Biennial Conference, Coastal and Estuarine Research Federation, 1-11 November, Virtual Conference. [Planned]

Miller, H.J., Conrad, J.R., Ward, E.J., Duberstein J.A., and Krauss, K.W., 2021, Water use efficiency of fertilized black (*Avicennia germinans*) and red (*Rhizophora mangle*) mangrove trees in south Florida, 2021 Water Resources Conference, 8-11 November, Kissimmee, Florida.

Ward, E.J., et al., 2021, Modeling tidal wetland carbon cycling in the USA using data from a range of spatiotemporal scales, 11th INTECOL International Wetlands Conference, 10-15 October, Christchurch, New Zealand, Virtual Conference. [Invited]

Buffington, K., Carr, J., MacKenzie, R.A., Apwong, M., Krauss, K.W., Guntenspergen, G.R., and Thorne, T., 2021, Mangrove responses to sea-level rise: Empirical datasets and process-based models to simulate alternative futures, 11th INTECOL International Wetlands Conference, 10-15 October, Christchurch, New Zealand, Virtual Conference. [Invited]

MacKenzie, R.A., Krauss, K.W., Cormier, N., Eperiem, E., van Aardt, J., and Karger, A.R., 2021, Monitoring mangrove response to sea level rise: ^{210}Pb, SETs, or LiDAR?, 26th Biennial Conference, Coastal and Estuarine Research Federation, 1-11 November, Virtual Conference.

Miller, H.J., Conrad, J.R., Ward, E.J., Duberstein J.A., and Krauss, K.W., 2021, Water use efficiency of fertilized black (*Avicennia germinans*) and red (*Rhizophora mangle*) mangrove trees in south Florida, 2021 Water Resources Conference, 8-11 November, Kissimmee, Florida.

Krauss, K.W., 2022, Science to inform the management of mangrove ecosystems undergoing sea level rise at Ding Darling National Wildlife Refuge, Sanibel Island, Florida, *Webinar*, Southeast Climate Adaptation Science Center, Raleigh, North Carolina, 19 January.

MacKenzie, R.A., Krauss, K.W., Thorne K., and Buffington, K., 2022, More effective management of mangroves as a nature-based solution, *Webinar*, Ridge to Reef Dialogue, US-Philippines Science and Technology Agreement Seminar, US Embassy, 7-8 March, Manilla, Philippines. [Invited]

Miller, H.J., Duberstein, J.A., Ward, E.J., Krauss, K.W., and Conrad, J.R., 2022, Water use and nutrient retention in fertilized black and red mangroves of Southwest Florida, Ecological Society of America Annual Meeting, 14-19 August, Montréal, Québec, Canada.

Krauss, K.W., 2022, Management of mangrove ecosystems undergoing sea-level rise: how the USGS and USFWS co-produced actionable adaptation outcomes, National Adaptation Forum, 25-27 October, Baltimore, Maryland.

MacKenzie, R.A., Krauss, K.W., Thorne, K.M., and Buffington, K.G., 2022, More effective management of mangroves as a nature-based solution, *Webinar*, Ridge to Reef Dialogue, US-Philippines Science and Technology Agreement Seminar, US Embassy, Manilla, Philippines, 7-8 March.

MacKenzie, R.A., Krauss, K.W., 2023, Why so blue carbon?, University of the Philippines, Manila, Philippines, 25 February.

Krauss, K.W., 2023, The blue carbon resource: budget and vulnerabilities, Blue Carbon Law Symposium, Sea Grant Law Center, University of Georgia, 17-18 May. [Invited]

Krauss, K.W., Ward, E.J., Merino, S., Miller, H., Duberstein, J.A., and Conrad, J.R., 2023, Net ecosystem exchange of CO_2 in mangroves: estimation from leaf, tree, and stand water use characteristics, 6th Mangrove Macrobenthos and Management (MMM6) Conference, 24-28 July, Cartagena, Colombia.

Buffington, K., Thorne, K., Krauss, K.W., MacKenzie, R.A., and Carr, J., 2023, Mangrove response to sea-level rise: projections of blue carbon and biodiversity from resilient and vulnerable ecosystems, 6th Mangrove Macrobenthos and Management (MMM6) Conference, 24-28 July, Cartagena, Colombia.

Lovelock, C.E., Carr, J., Friess, D.A., Guntenspergen, G.R., Krauss, K.W., Marchand, C., Pearse, A., and Swales, A., 2023, Trends in sediment surface elevation of tropical mangroves vary among geomorphic settings, 6th Mangrove Macrobenthos and Management (MMM6) Conference, 24-28 July, Cartagena, Colombia.

Zhu, Z., Yang, X., Zhu, Z., Krauss, K.W., and Ward, E.J., 2023, Tracking loss and recovery of mangrove forests from repeat hurricanes using Landsat. 6th Mangrove Macrobenthos and Management (MMM6) Conference, 24-28 July, Cartagena, Colombia.

Water use by trees and stands in tidal swamps and mangroves: improving our insights on stress physiology and water conservation, 2023, Xi Sigma Pi Apple Pie Seminar Series, School of Renewable Natural Resources, Louisiana State University, 24 October, Baton Rouge, LA.

References Cited (Appendices)

Aké-Castillo, J.A., Vázquez, G., and López-Portillo, J., 2006, Litterfall and decomposition of *Rhizophora mangle* L. in a coastal lagoon in the southern Gulf of Mexico: Hydrobiologia, v. 559, p. 101–111.

Buffington, K.J., and Thorne, K.M., 2019, LEAN-corrected Collier County DEM for wetlands: U.S. Geological Survey data release, https://doi.org/10.5066/P9GJFZHT.

Buffington, K.J., MacKenzie, R.A., Carr, J.A., Apwong, M., Krauss, K.A., and Thorne, K.M., 2021, Mangrove species' response to sea-lever rise across Pohnpei, Federated States of Micronesia: Reston, Open-File Report 2021-1002.

Castañeda-Moya, E., Twilley, R.R., Rivera-Monroy, V.H., Marx, B.D., Coronado-Molina, C., and Ewe, S.M.L., 2011, Patterns of root dynamics in mangrove forests along environmental gradients in the Florida Coastal Everglades, USA: Ecosystems, v. 14, 1178–1195.

Chen, G., Hong, W., Gu, X., Krauss, K.W., Zhao, K., Fu, H., Chen, L., Wang, M., and Wang, W., 2023. Coupling near-surface geomorphology with mangrove community diversity at the estuarine scale: a case study at Dongzhaigang Bay, China: Sedimentology, v. 70, p. 31–47.

Chen, R., and Twilley, R.R., 1999, A simulation model of organic matter and nutrient accumulation in mangrove wetland soils: Biogeochemistry, v. 44, p. 93–117.

Conrad, J.R., 2022, The effects of nutrient inputs on surface elevation change processes in tidal mangrove forests: Boca Raton, Florida Atlantic University, Ph.D. dissertation.

Drexler, J., 2019, Dry weight, volume and % organic carbon in mangrove sediment cores collected in September 2018 in J.N. "Ding" Darling National Wildlife Refuge, Sanibel Island, Florida, United States: U.S. Geological Survey data release. https://doi.org/10.5066/P9CFK79S.

Faron, N.T., 2021, The impact of nutrient loading on the soil and root respiration rates of Florida mangroves: Boca Raton, Florida Atlantic University, M.S. thesis.

Kirwan, M.L., Guntenspergen, G.R., D'Alpaos, A., Morris, J.T., Mudd, S.M., and Temmerman, S., 2010, Limits on the adaptability of coastal marshes to rising sea level: Journal of Geophysical Research, v. 37, L23401.

Kirwan, M.L., Temmerman, S., Skeehan, E.E., Guntenspergen, G.R., and Fagherazzi, S., 2016, Overestimation of marsh vulnerability to sea level rise: Nature Climate Change, v. 6, p. 253–260.

Krauss, K.W., McKee, K.L., Lovelock, C.E., Cahoon, D.R., Saintilan, N., Reef, R., and Chen L., 2014, How mangrove forests adjust to rising sea level: New Phytologist, v. 202, p. 19–34.

Krauss, K.W., Duberstein, J.A., and Conner, W.H., 2015, Assessing stand water use in four coastal wetland forests using sapflow techniques: annual estimates, errors and associated uncertainties: Hydrological Processes, v. 29, p. 112–127.

McKee, K.L., 2011, Biophysical controls on accretion and elevation change in Caribbean mangrove ecosystems: Estuarine, Coastal and Shelf Science, v. 91, p. 475–483.

McKee, K.L., Cahoon, D.R., and Feller, I.C., 2007, Caribbean mangroves adjust to rising sea level through biotic controls on change in soil elevation: Global Ecology and Biogeography, v. 16, p. 545–556.

Middleton, B.A., and McKee, K.L., 2001, Degradation of mangrove tissues and implications for peat formation in Belizean island forests: Journal of Ecology, v. 89, p. 818–828.

Miller, H., 2022, Water use and nutrient retention in fertilized black and red mangroves in southwest Florida: Clemson, Clemson University, M.S. thesis.

Peneva-Reed, E.I., Zhu, Z., 2019. Mangrove data collected from J.N. "Ding" Darling National Wildlife Refuge, Sanibel Island, Florida, United States: U.S. Geological Survey data release. https://doi.org/10.5066/P9P2PHU3.

Peneva-Reed, E.I., Krauss, K.W., Bullock, E.L., Zhu, Z., Woltz, V.L., Drexler, J.Z., Conrad, J.R., and Stehman, S.V., 2021, Carbon stock losses and recovery observed for a mangrove ecosystem following a major hurricane in Southwest Florida: Estuarine, Coastal and Shelf Science, v. 248, 106750.

Rogers, K., Kelleway, J.J., Saintilan, N., Megonigal, J.P., Adams, J.B., Holmquist, J.R., Lu, M., Schile-Beers, L., Zawadzki, A., Mazumder, D., and Woodroffe, C.D., 2019, Wetland carbon storage controlled by millennial-scale variation in relative sea-level rise: Nature, v. 567, p. 91–95.

Simpson, L.T., Chapman, S.K., Simpson, L.M., and Cherry, J.A., 2023, Do global change variables alter mangrove decomposition? A systematic review: Global Ecology and Biogeography, v. 32, p. 1874–1892.

Snedaker, S.C., 1995: Mangroves and climate change in the Florida and Caribbean region: scenarios and hypotheses: Hydrobiologia, v. 295, p. 43–49.